Energy Materials and Devices

Review

Porous zinc metal anodes for aqueous zinc-ion batteries: Advances and prospectives

Yichen Ding, Bingyue Ling, Xin Zhao, Xu Yang, Yao Wang ✉, Dong Zhou ✉, and Guoxiu Wang ✉

Graphical Abstract

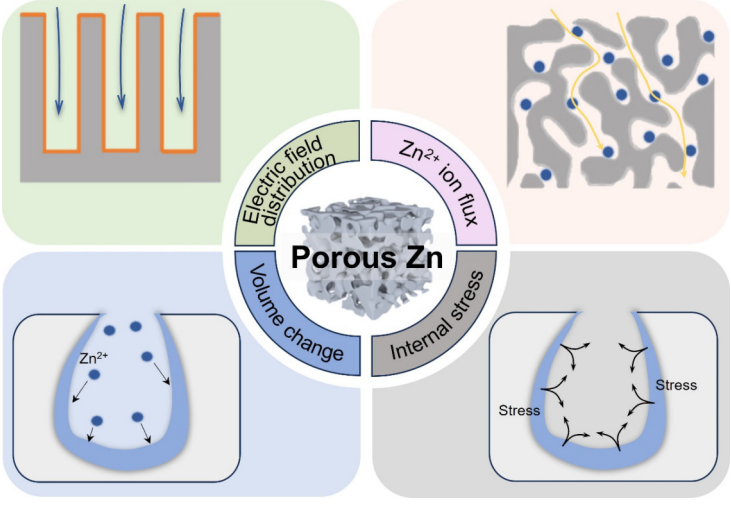

The failure of Zn metal anodes in aqueous zinc-ion batteries is highly related to excessive dendrite growth. The implementation of porous Zn anodes has been demonstrated to be an effective strategy to regulate the deposition/stripping behavior of Zn^{2+} ions, thereby inhibiting the growth of Zn dendrites. This review provides a comprehensive overview of the recent advancements in the engineering of porous Zn metal anodes, emphasizing the structural orderliness and summarizing the merits of porous Zn anodes.

✉Address correspondence to
Yao Wang,
ywang99@sz.tsinghua.edu.cn;
Dong Zhou,
zhou.d@sz.tsinghua.edu.cn;
Guoxiu Wang,
Guoxiu.Wang@uts.edu.au

Received: May 6, 2024
Revised: May 23, 2024
Accepted: May 26, 2024

Read Online

Submit Online

Citation: Ding Y., Ling B., Zhao X., et al. Porous zinc metal anodes for aqueous zinc-ion batteries: Advances and prospectives. *Energy Mater. Devices*, 2024, 2(3), 9370040. https://doi.org/10.26599/EMD.2024.9370040

Energy Materials and Devices

Open Access

Review

https://doi.org/10.26599/EMD.2024.9370040

Porous zinc metal anodes for aqueous zinc-ion batteries: Advances and prospectives

Yichen Ding[1,†], Bingyue Ling[1,†], Xin Zhao[1], Xu Yang[2], Yao Wang[1] ✉, Dong Zhou[1] ✉, and Guoxiu Wang[2] ✉

[1] *Tsinghua Shenzhen International Graduate School, Tsinghua University, Shenzhen 518055, China*

[2] *Center for Clean Energy Technology, School of Mathematical and Physical Sciences, Faculty of Science, University of Technology Sydney, Sydney 2007, Australia*

[†] *Yichen Ding and Bingyue Ling contributed equally to this work.*

Received: May 6, 2024 / **Revised:** May 23, 2024 / **Accepted:** May 26, 2024

ABSTRACT

The intensifying challenges posed by climate change and the depletion of fossil fuels have spurred concerted global efforts to develop alternative energy storage solutions. Aqueous zinc-ion batteries (AZIBs) have emerged as promising candidates for large-scale electrochemical energy storage systems because of their intrinsic safety, cost-effectiveness, and environmental sustainability. However, Zn dendrite growth consistently poses a remarkable challenge to the performance improvement and commercial viability of AZIBs. The use of three-dimensional porous Zn anodes instead of planar Zn plates has been demonstrated as an effective strategy to regulate the deposition/stripping behavior of Zn^{2+} ions, thereby inhibiting the dendrite growth. Here, the merits of porous Zn anodes were summarized, and a comprehensive overview of the recent advancements in the engineering of porous Zn metal anodes was provided, with a particular emphasis on the structural orderliness and critical role of porous structure modulation in enhancing battery performance. Furthermore, strategic insights into the design of porous Zn anodes were presented to facilitate the practical implementation of AZIBs for grid-scale energy storage applications.

KEYWORDS

aqueous zinc-ion battery, porous zinc metal anode, dendrite, structural orderliness, grid-scale energy storage.

1 Introduction

The depletion of fossil energy sources can no longer satisfy the growing energy demands of humanity, which exacerbates numerous irremediable environmental issues[1]. In mitigating these challenges, renewable energy sources (e.g., wind, solar, and tidal) have received considerable attention because of their abundance and environmental friendliness. However, the integration of these energy sources into the electrical grid, constrained by indirectness and geographic limitations, can disrupt the stability of electrical energy storage systems, highlighting the demand for the development of efficient and sustainable energy storage technologies[2–4]. Electrochemical batteries, which are renowned for their inherent reliability and high energy conversion efficiency, stand out as an optimal solution for electrical energy conversion and storage[5]. Therefore, the demand for secondary battery systems that are cost-effective, safe, and eco-friendly is increasing. Lithium-ion batteries (LIBs) are widely used in electric vehicles and consumer electronics because of their high energy density and long cycle life. However, the increasing costs associated with limited lithium mineral resources, in addition to persistent safety concerns, have hindered their widespread adoption in stationary grid energy storage systems[6]. In this context, aqueous zinc-ion batteries (AZIBs) with Zn metal

✉Address correspondence to Yao Wang, ywang99@sz.tsinghua.edu.cn; Dong Zhou, zhou.d@sz.tsinghua.edu.cn; Guoxiu Wang, Guoxiu.Wang@uts.edu.au

© The Author(s) 2024. Published by Tsinghua University Press. The articles published in this open access journal are distributed under the terms of the Creative Commons Attribution 4.0 International License (http://creativecommons.org/licenses/by/4.0/), which permits use, distribution and reproduction in any medium, provided the original work is properly cited.

anodes, which were first proposed by Kang et al. in 2012[7], have attracted increasingly interests in recent years because of their relatively high theoretical capacity (820 mAh g^{-1} and 5,855 mAh cm^{-3}), relatively low redox potential (−0.762 V vs. standard hydrogen electrode), and low cost of Zn metal[8]. Moreover, compared with their organic counterparts, aqueous electrolytes provide inherent safety, superior ionic conductivity, and cost-effectiveness, thereby indicating their great potential for large-scale energy storage applications.

Despite their potential, AZIBs remain in an early stage of development, with challenges such as dendrite growth and side reactions (e.g., corrosion, passivation, and hydrogen precipitation reactions), thereby hindering their commercialization[9]. Notably, the formation of Zn dendrites poses a critical risk because of their propensity to penetrate the separator, leading to direct contact between the cathode and anode, which triggers internal short circuits and cell failure[10,11]. Numerous strategies have been used to inhibit the dendrite growth, including electrolyte and additive design[12–14], anode surface modification[15], and anode structural engineering. Among these, the development of porous structures has emerged as an effective approach to regulate the stripping/plating behavior of Zn metal and prevent dendrite growth, leveraging their capability of homogenizing the electric field distribution and ion flux, mitigating volume expansion, and releasing the internal stresses associated with Zn deposition[10]. Various porous fabrication techniques have been applied, including etching[16], self-assembly[17], laser lithography[18], electrochemical methods[19], rolling[20], freeze drying[21], and three-dimensional (3D) printing[22]. Although extensive research has been conducted on porous Zn electrodes to enhance battery performance, spanning from Zn sponges to gradient electrodes (Fig. 1), systematic analysis from the perspective of the structural orderliness of the porous architecture remains lacking.

Herein, a comprehensive summary of the research advances in porous Zn anode design for AZIBs was provided, elucidating the role of porous structures in the overall battery performance, particularly the precise regulation of the pore structure. In addition, Zn powder-based anodes, which have been largely overlooked in previous reviews, were comprehensively overviewed. This review aims to provide novel insights and strategic guidance for the development of high-performance AZIBs through the optimization of porous Zn anodes.

2 Merits of porous Zn anodes

Although commercial planar Zn foils can serve as anodes for AZIBs, the uneven distribution of charge

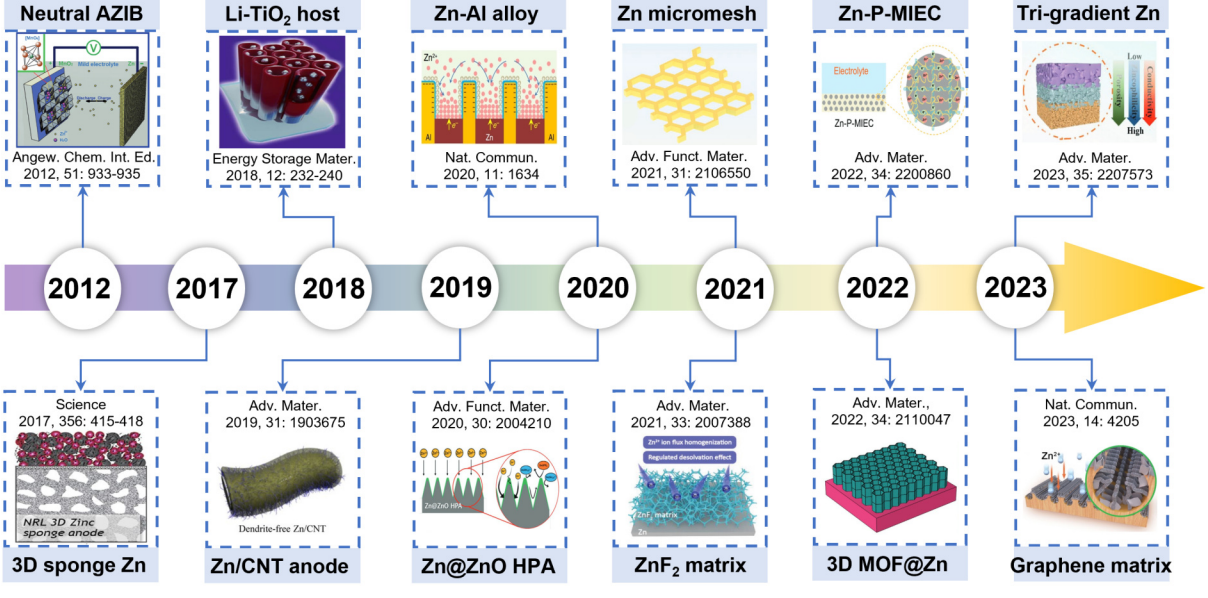

Figure 1 Timeline of the development of porous Zn anodes in AZIBs. Reproduced from Ref. [7] with permission ©2012, Wiley-VCH Verlag GmbH & Co. KGaA, Weinheim. Reproduced from Ref. [23] with permission ©2017, American Association for the Advancement of Science. Reproduced from Ref. [24] with permission ©2018, Elsevier B.V. Reproduced from Ref. [25] with permission ©2019, Wiley-VCH Verlag GmbH & Co. KGaA, Weinheim. Reproduced from Ref. [26] under the CC BY 4.0 license ©2020, The Authors. Reproduced from Ref. [27] with permission ©2020, Wiley-VCH Verlag GmbH & Co. KGaA, Weinheim. Reproduced from Ref. [28] with permission ©2021, Wiley-VCH GmbH. Reproduced from Ref. [29] with permission ©2021, Wiley-VCH GmbH. Reproduced from Ref. [30] with permission ©2022, Wiley-VCH GmbH. Reproduced from Ref. [21] with permission ©2022, Wiley-VCH GmbH. Reproduced from Ref. [31] with permission ©2023, Wiley-VCH GmbH. Reproduced from Ref. [32] under the CC BY 4.0 license ©2023, The Authors.

density and cation concentration disrupts Zn deposition and stripping, leading to dendrite growth and impeding the practical application of AZIBs. By contrast, 3D porous anodes provide numerous nucleation sites and reduce nuclear energy barriers because of their enlarged electrochemically active area. This enhancement greatly mitigates the localized charge accumulation, facilitates the uniform electric field distribution and mass transport, suppresses the dendrite growth, and ensures a longer battery lifespan. Moreover, the substantial internal volume in 3D porous anodes can accommodate volume changes and deposition stress caused by deposition/stripping. In particular, 3D porous anodes exhibit four main merits (Fig. 2).

2.1 Uniform electric field distribution

Electric field distribution plays a pivotal role in affecting the deposition behavior of Zn ions. According to the space charge theory proposed by Chazalviel et al., anion depletion is induced when the mass flux surpasses a threshold, compelling anions to migrate away from the anode[33]. Sand's temporal model provides an approximation of the time (τ_s) required for anion depletion, which leads to the formation of a space charge region caused by the disruption of localized electroneutrality. This phenomenon results in a large electric field-driven electroconvection on the metal surface, thereby exacerbating dendrite growth[34]. In general, this model is grounded on a high mass-transport-limited current density[33,35]. However, experimental results reveal that the duration of dendrite growth at low current densities is consistent with the predictions of the Sand's model, indicating a strong correlation between dendrite formation and the ion concentration gradient on the electrode surface[35]. On planar Zn foils, the restricted ion transport exacerbates the concentration of electric field distribution, resulting in localized high current densities that aggravate side reactions and accelerate AZIB degradation. By contrast, 3D porous electrodes provide an increased number of electrochemically active surfaces and abundant nucleation sites that contribute to a more uniform electric field distribution, thereby extending τ_s associated with the formation of space charge layers[10].

2.2 Homogeneous ion flux

The transport of Zn^{2+} ions remarkably affects the electrochemical deposition behavior and morphology of the electrode surface[36]. However, the uneven and rough surface of planar Zn foils results in the accumulation of negative charges at the bumps, resulting in a "tip effect" that induces the preferential deposition of Zn ions and fosters dendrite growth. The ionic electrochemical kinetics at the anode surface includes the migration of metal ions across the concentration gradient in the electrolyte and the charge transfer at the electrode–electrolyte interface[37]. Herein, ion diffusion resistance plays a key role, which follows the Nernst–Planck equation[38]:

$$J_i = -D_i \frac{dC_i}{dx} - u_i c_i z_i F \frac{dv}{dx} \quad (1)$$

where J denotes the ion flux, D is the diffusion coefficient, C represents the ion concentration, u is the ion mobility, z signifies the number of electrons, F is the Faraday constant, and V is the voltage. The first term of the Nernst–Planck equation describes ion diffusion, whereas the second term corresponds to ion mobility under an electric field. At high current densities, ion diffusion dominates because of substantial concentration gradients in Zn ion. In 3D porous electrodes, the electrolyte penetrates deeply into the electrode, and an increased electrochemically active area effectively reduces the local current density and mitigates the concentration polarization

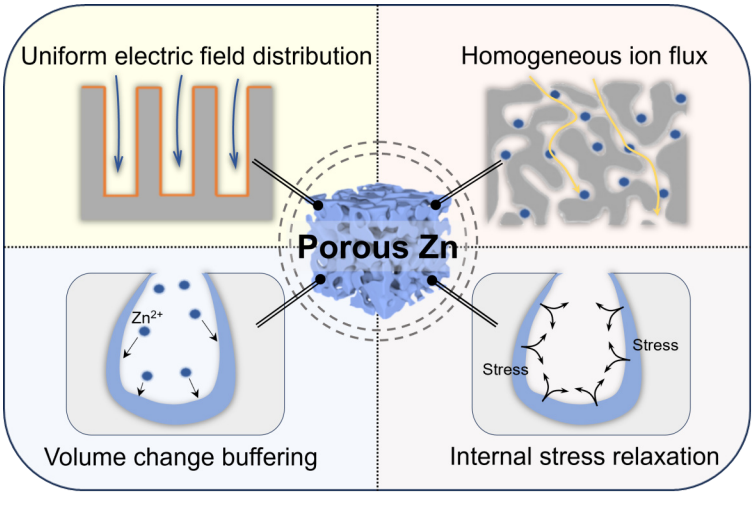

Figure 2 Advantages of porous structured Zn metal anodes, including uniform electric field distribution, homogeneous ion flux, buffering volume change, and internal stress relaxation.

清華大學出版社 Tsinghua University Press | SciOpen

of the electrolyte, thereby reducing the ion diffusion resistance and facilitating a homogeneous ion flux. Moreover, the abundance of nucleation sites effectively lowers the nucleation energy barrier and increases the deposition overpotential, thereby enabling rapid and uniform deposition[39].

2.3 Volume change buffering

The hostless feature of Zn metal leads to vigorous volume swelling and shrinking during repeated plating/stripping[20]. The nonuniform distribution of charge and ion flux on planar Zn metal surfaces induces uneven Zn deposition. Hence, Zn metal is prone to being deposited in dendritic, mossy, and rod-like forms, which lead to substantial volume changes that exacerbate dendritic growth. In addition, the increased specific surface area and decreased lattice match caused by volume expansion can lead to the disordered deposition of Zn, thereby reducing the lifetime of AZIBs[40]. The substantial volume changes in planar Zn foil anode systems lead to the formation of "dead Zn" and the puncture of separator by dendrites[41]. The construction of porous Zn metal anodes can provide a sufficient internal space to effectively accommodate the volume change of Zn metal and inhibit dendrite growth. A well-designed porous anode can induce Zn to achieve bottom-up deposition behavior and maintain a flat electrode sheet morphology[26].

2.4 Internal stress relaxation

Internal stresses arise during Zn deposition, which could affect the deposition behavior[42]. Under nonequilibrium growth conditions, the migration of Zn metal atoms across grain boundaries is a decisive factor influencing the accumulation of internal stresses[10]. In planar electrodes, these stresses are not effectively released, leading to the chaotic deposition behavior of Zn atoms along the grain boundaries, which drives the growth of a disordered dendritic metal structure. By contrast, porous structures can effectively alleviate the internal stress induced by metal deposition, thereby facilitating an orderly deposition process for Zn.

3 Porous Zn anodes with a disordered structure

Prior to the burgeoning interest in mild AZIBs, monolithic porous Zn anodes had been investigated in alkaline Zn batteries, which focused on Zn sponge and Zn foam structures. In 2017, Parker et al. designed porous Zn sponge electrodes to improve Zn utilization and charging capacity[23]. This design effectively modulated the local current density to retard dendrite formation. Zn foam, which plays a similar role to Zn sponge, has been used as an anode to enhance battery performance by modulating the electric field[43]. In another work, a hyper-dendritic nanoporous Zn foam was developed via *in situ* electrochemical synthesis[44]. This Zn foam achieved an impressive anode material utilization of ~100% at 100% depth of discharge (DOD) in an alkaline medium. However, the structures of Zn sponge and Zn foam are susceptible to structural collapse after long-term high-rate cycling, and their fabrication generally requires great energy expenditure, which hinders their practical applications. In the study of neutral AZIBs, random porous Zn anodes have been developed to enhance the anode-to-cathode reversible capacity ratio (N/P ratio), specific capacity, cycle life, and rate performance. At present, the realization of porous Zn anodes is achieved through three main methods, that is, the *in situ* creation of pores on commercial Zn foils, the deposition of Zn on 3D zincophilic substrates, and the construction of porous structures utilizing the plasticity of Zn powders.

3.1 Zn foil anodes with a disordered structure

The surface of commercial Zn foils is rough, and it lacks planarity, which can induce the accelerated formation of Zn dendrites. The *in situ* construction of a porous layer on the surface of Zn foils reduces the local current density, homogenizing the ion flux and inhibiting the dendrite growth. Compared with alternative methods for fabricating 3D anodes, direct etching of commercial Zn foils using simple processes such as immersion and ultrasonic waves shows great application potential. This etching process not only eliminates the original passivation layer on the surface of Zn foils, but also establishes a 3D structure. Meanwhile, under specific conditions, Zn compounds can be generated *in situ* on the surface of Zn foils, self-assembling into an interfacial layer to protect the Zn anode. Notably, the structural morphology and etching dynamics of Zn foils vary with the etchant and etching parameters used. Given the formation of a porous structure, further enhancements can be achieved by manipulating the crystal orientation[40,45–47] and by forming protective layers composed of Zn compounds or inert metals on the surface.

Acid solutions serve as effective etching agents for Zn foils, facilitating the redox reaction where Zn atoms react with hydrogen ions (ionized by the acid), to form the corresponding Zn salts and hydrogen. In addition, if the acid's anion can coordinate, then it can bind with Zn^{2+} to regulate the flux, and the resulting coordination compounds generated *in situ* can serve as a protective layer to reduce corrosion. As demonstrated by Sun et al., hydrochloric acid was utilized to selectively etch the crystal surface of Zn foils, forming a 3D ridge-like structure[48]. This engi-

neered surface of the Zn electrode facilitated the uniform plating and stripping of metal Zn, which increased the infiltration surface area of the electrolyte and reduced the local current density, thereby improving the cycling stability of the Zn anode. Organic acids, which are less aggressive than their inorganic counterparts, provide a gradual and controllable etching process for Zn foils. Different organic acids, including phytic acid[49], humic acid[50], amino acid[51], and cysteine[16,52], have been used to fabricate porous Zn anodes. A 3D Zn foil with a hierarchical porous structure was developed by Alshareef et al. using an organic mixed solution of trifluoromethanesulfonic acid (TFA) and acetonitrile[53]. TFA with a relatively slow and controllable chemical corrosion of Zn effectively removed the surface passivation layer (Fig. 3a), resulting in a multitude of porous structures with diameters ranging from nanoscale to microscale on the Zn surface. This solution improved the electrolyte accessibility and nucleation site density. Organic acids, with their reactive groups, provide abundant adsorption sites for metal ions, forming exceptionally stable complexes with Zn ions[58]. Consequently, the etched Zn foil surface can generate organic Zn compounds *in situ* as a protective interface layer, reducing the electrolyte–Zn anode contact and effectively preventing the corrosion of the Zn foil surface by O_2 or water.

Zn foil etching using metal salt solutions as etchants is also a feasible strategy, where the metal salt solution facilitates the formation of a porous inert protective film on the surface of Zn foils

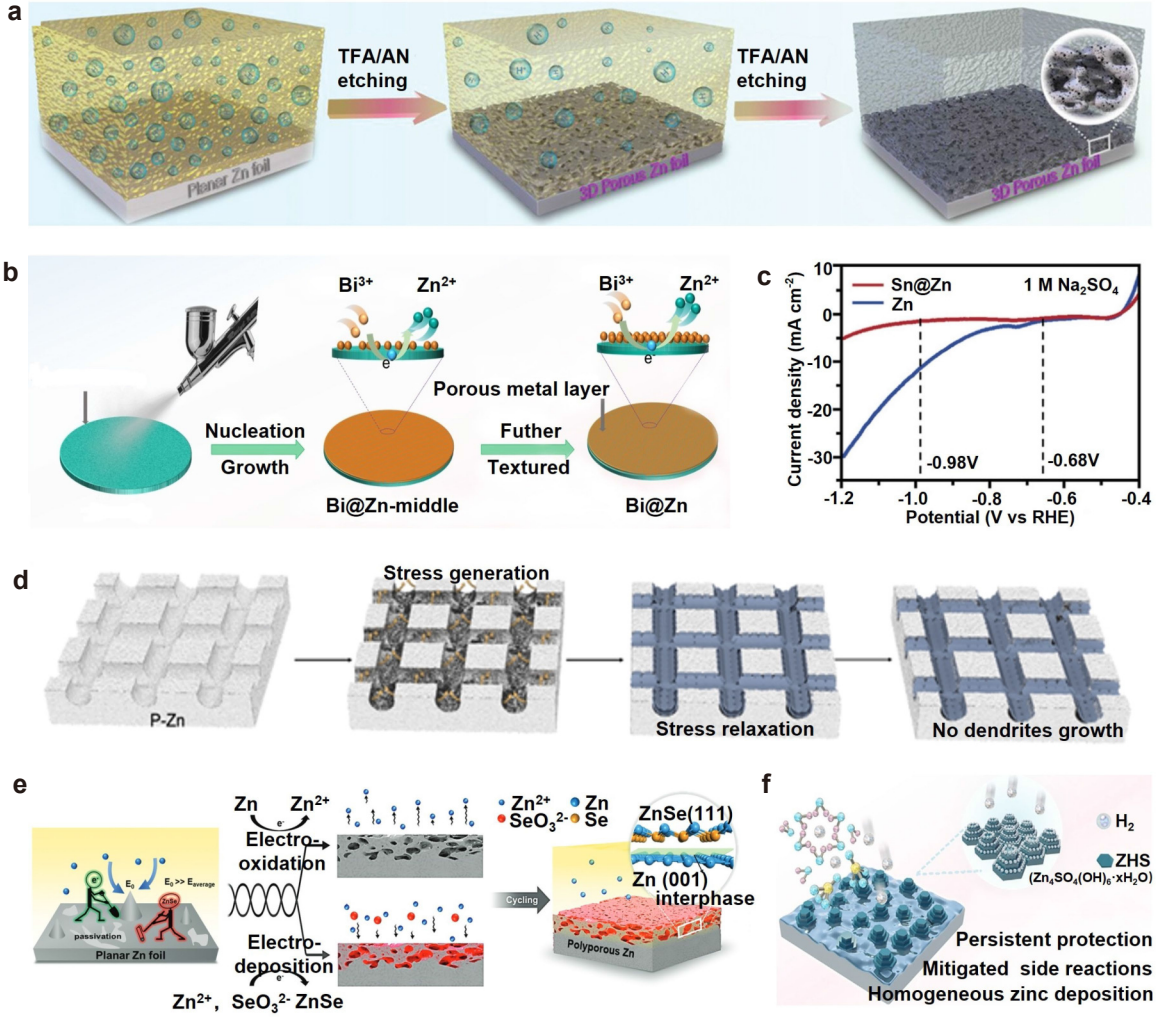

Figure 3 Zn foil anodes with a disordered structure. (a) Schematic diagram showing the fabrication of a 3D porous Zn foil in an organic mixture of trifluoromethanesulfonic acid (TFA) and acetonitrile (AN). Reproduced from Ref. [53] with permission ©2022, Wiley-VCH GmbH. (b) Schematic depiction of the fabrication and formation of Zn anodes with a metallic interface. Reproduced from Ref. [54] with permission ©2023, Wiley-VCH GmbH. (c) Line sweep voltammetry curves of pristine Zn and Sn@Zn electrodes at 1 mV s^{-1} (using 1 mol/L $NaSO_4$). Reproduced from Ref. [55] with permission ©2023, Wiley-VCH GmbH. (d) Schematic illustration of the stress induced by Zn plating and its effect on the plating/stripping behavior of Zn on P–Zn. Reproduced from Ref. [56] with permission ©2022, Elsevier Ltd. (e) Schematic illustration of the preparation of the 3D-Zn@ZnSe anode under constant potentials. Reproduced from Ref. [57] with permission ©2022, Wiley-VCH GmbH. (f) Schematic diagram of Zn deposits on a ZnCo alloy surface. Reproduced from Ref. [19] with permission ©2023, Wiley-VCH GmbH.

through a simple redox reaction between metal ions and Zn. By introducing zincophilic metals with high hydrogen evolution potentials, the Zn anode demonstrated improved deposition behavior of Zn^{2+} for drastically increased cycling stability[59].

Notably, studies have shown that the inert metal deposited on the Zn foil surface during cycling can be electrochemically converted into Zn alloys, which exhibit superior oxidation resistance and load-bearing capacity compared with pure metal Zn. Chao et al. optimized zincophilic sites from thermodynamic inertia and kinetic zincophilicity indices by using $BiCl_3$ and ethylene glycol solvent to form *in situ* nanoporous Bi@Zn nanosheets on Zn foils (Fig. 3b)[54]. The Bi@Zn interface greatly suppressed the side reactions. The *in situ* formed Zn–Bi alloy solid solution interfaces spatially promoted the homogeneous growth of Zn and effectively accelerated the Zn deposition kinetics. Given the high thermodynamic inertia and rapid electrochemical kinetic zincophilicity, the Bi@Zn heterometallic interface enabled a long cycle lifespan of more than 4,700 cycles with a low overpotential of around 55 mV, even at a high current density of 10 mA cm^{-2}. In addition, Wu et al. reported a versatile and economical strategy for constructing artificial metal interfaces on Zn anodes within only 10 s[55]. The kinetic process of replacement reaction was regulated by the complexation of thiourea molecules with metal ions, and the metal deposition was gradually adjusted, achieving superfilling on the surface of common commercial Zn flakes. As shown in Fig. 3c, the hydrogen evolution reaction (HER) onset potential of Sn@Zn (−0.98 V vs. reversible hydrogen electrode) was lower than that of Zn (−0.68 V), indicating the sluggish HER response of Sn@Zn with regard to current density. Considering the evaluated parameters such as surface morphology, interfacial resistance, corrosion current, and nucleation overpotential, Sun et al. selected $MoCl_5$/ethanol etchant from high-valent metal chlorides for the *in situ* construction of porous Zn surfaces[60]. Electrochemical analyses and theoretical calculations showed that an increased exposure of the Zn(002) crystal plane enhanced the corrosion resistance of the anode.

The corrosion mechanism of Zn foils exposed to metallic salt solutions can be summarized in three key aspects: (1) The selective adsorption of different anions to the Zn metal crystal surface induces the oriented deposition of Zn^{2+} ions[61]. (2) Once an inert metal or compound is *in situ* substituted on the surface of the Zn foil, it functions as a protective barrier to isolate the Zn anode from the electrolyte and improves the corrosion resistance of the Zn anode because of its chemical inertness[62,63]. (3) Under certain conditions, the deposited inert metal on the surface can spontaneously alloy with Zn, thereby improving the corrosion resistance and ensuring the structural stability of the battery during cycling[54]. Notably, the concentration and duration of the metal salt solution remarkably influence the particle size and thickness of the deposited metal layer[64].

The growth of Zn dendrites is closely related to the accumulation of internal stresses during the electroplating process. Thus, Zn metal anodes with a patterned micro-groove structure have been demonstrated to effectively release the stress induced by galvanization, thereby inhibiting dendrite growth. Zhao et al. adopted micro-zone stress relaxation to introduce ordered grooves (~30 μm wide and ~25 μm deep) to the surface of Zn metal foils (P–Zn) by metal mesh-assisted rolling, which inhibited Zn dendrite growth (Fig. 3d)[56]. The post-patterned recesses provided a sufficient buffer space to effectively reduce stress accumulation from plating, enabling dendrite-free Zn metal plating even at a high capacity of 10 mAh cm^{-2}. Apart from physical imprinting and chemical etching, some electrochemical methods are available to fabricate intricate porous structures on the surface of Zn foils. The uneven deposition of Zn can be attributed to various factors[65], including surface roughness, passivation, the "tip effect", as well as inhomogeneous ion fluxes in the electrolyte. Zhi et al. successfully obtained a 3D porous Zn skeleton with a ZnSe overlayer (3D-Zn@ZnSe) through one-step electrochemical scanning, accurately repairing intrinsic defects on the surface of Zn foils and remodeling the electrolyte–anode interface[57]. Under a certain electric field, the preferential reaction at protrusions caused by a higher surface current density facilitated the simultaneous electrooxidation of Zn and the electrodeposition of ZnSe in a SeO_2 powder-rich electrolyte (Fig. 3e). The anode–electrolyte interface was reconfigured, effectively homogenizing the charge distribution and Zn ion flux; thus, the 3D-Zn@ZnSe||V_2O_5 cells exhibited 90.63% capacity retention after 8,500 cycles at 5 A g^{-1}, which maintained a high specific capacity of 107.3 mAh g^{-1}. Zhou et al. designed a novel approach to fabricate spiral-grown 3D ZnCo overlayers on one side of commercial Zn foils using constant current electrodeposition. The ZnCo crystalline plane, which is predominantly exposed to the side of the 3D spiral structure, had enhanced zincophilicity compared with the Zn crystalline plane[19]. During electroplating, the Zn metal surface with a ZnCo cladding layer was gradually smoothed because of the restricted diffusion behavior of Zn^{2+}. Meanwhile, the superior corrosion resistance of ZnCo alloy effectively inhibited the corrosion reaction on the anode surface (Fig. 3f).

Overall, the fabrication of random porous structures on the surface of commercial Zn foils through

physical, chemical, or electrochemical methods represents a feasible yet effective strategy to improve the performance of AZIBs. These porous structures can effectively optimize ion flux, inhibit side reactions, and regulate Zn nucleation growth. However, the efficacy of the modification approach is highly contingent on the reaction conditions because of the inherent variability in the size and arrangement of pore structures. Thus, a more in-depth investigation into the impact of the characteristics of a porous structure on the Zn deposition/stripping kinetics is warranted to optimize the performance of AZIBs.

3.2 Current collectors with a disordered structure

3.2.1 Metallic current collectors with a disordered structure

Metal materials, which are known for their high electrical conductivity, thermal conductivity, and good ductility, are considered optimal candidates for battery current collectors. In addition, metal substrates typically exhibit zincophilic properties, which facilitates the deposition of Zn^{2+} ions onto them.

Among numerous metals, copper stands out because of its relatively low cost, excellent conductivity, and low Zn nucleation overpotential. Huang et al. scrutinized the nucleation behavior of Zn on different metal substrates (e.g., Cu, Ag, Ti, or Sn), revealing that Zn tends to deposit on the surface of Cu in the absence of nucleation barriers[66]. Therefore, copper is a favorable material for Zn anode current collectors. 3D Cu used for Zn anode current collectors has two types, namely, modified commercial copper foil and direct porous copper, such as copper mesh and copper foam[67]. Kang et al. prepared 3D porous Cu from a flat Cu foil via chemical etching (Fig. 4a), providing a substrate for the uniform electrodeposition of Zn [68]. In addition, foam Cu can be used directly to obtain porous structures, as demonstrated by Shi et al.[69]. The 3D porous foam Cu exhibited a low Zn nucleation overpotential of 65.2 mV and superior plating/stripping reversibility, leading to enhanced cycling performance in the assembled

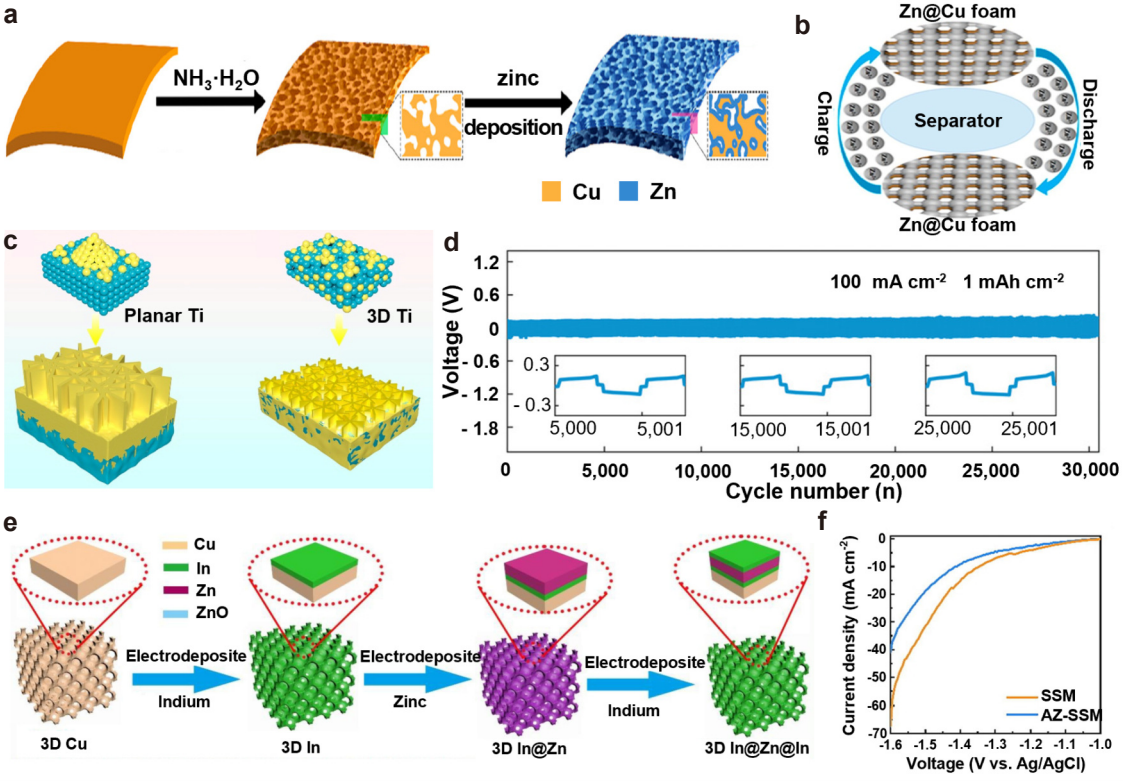

Figure 4 Metallic current collectors with a disordered structure. (a) Schematic illustration of the fabrication of a 3D Zn anode. Reproduced from Ref. [68] with permission ©2019, American Chemical Society. (b) Schematic illustration of Zn@Cu collector symmetric cells. Reproduced from Ref. [69] with permission ©2019, American Chemical Society. (c) Zn deposition diagram representing planar Ti and 3D Ti current collectors. Reproduced from Ref. [70] with permission ©2021, American Chemical Society. (d) Long-term stripping/plating behavior of Zn@CuNWs||Zn@CuNWs symmetric cells at a current density of 100.0 mA cm^{-2} with an areal capacity of 1.0 mAh cm^{-2}. Reproduced from Ref. [71] with permission ©2022, Wiley-VCH GmbH. (e) Scheme of the synthesis of a 3D porous sandwich-structured In@Zn@In (3D In@Zn@In) electrode. Reproduced from Ref. [72] with permission ©2022, Elsevier B.V. (f) Linear polarization curves of symmetric SSM and AZ-SSM electrodes in a 2 mol/L aqueous Na_2SO_4 electrolyte. Reproduced from Ref. [73] with permission ©2022, Science Press and Dalian Institute of Chemical Physics, Chinese Academy of Sciences.

full cell (Fig. 4b). Apart from Cu, other metals are also viable as anode current collector hosts. For example, An et al. developed 3D porous Ti derived from commercial Ti foil as a host for the anode[70]. The 3D Ti/Zn metal anode suppressed dendrite growth because of its uniform current distribution (Fig. 4c), homogeneous nucleation, and volume change accommodation, enabling stable Zn plating/stripping for up to 2,000 h with low polarization. The full cell with Zn@3D Ti–TiO_2 as the anode and S@MXene@MnO_2 as the cathode was assembled to evaluate the practical electrochemical performance. The cyclic voltammetry (CV) curves after the initial cycle displayed consistent redox peaks, indicating the reversibility of the electrochemical process.

Certain metals with unique structures have been utilized as anode current collectors. For example, Yi et al. have successfully used a fivefold twin-crystal Cu nanowire as a substrate for Zn anodes[71]. The regular Cu(111) crystal facets exposed at the ridges of these nanowires could regulate the growth of Zn dendrites because of their low lattice mismatch between Cu(111) and Zn(002). This heteroepitaxial growth method allowed Zn to be deposited along the Zn(002) orientation, in alignment with Cu(111), guiding uniform Zn nucleation and growth, and remarkably reducing the overpotential. Consequently, the Zn@CuNW anode exhibited unprecedented stability under ultra-high current density, as evidenced by symmetric cell operations exceeding 30,000 cycles at the rate of 100.0 mA cm^{-2} (Fig. 4d). A sandwich-like architecture has also been adopted for metallic anode current collectors. Fan et al. reported a distinctive In@Zn@In tri-layer structure deposited on the 3D porous Cu framework (referred to as 3D In@Zn@In), which effectively suppressed dendrite growth and side reactions (Fig. 4e)[72]. The sandwich configuration not only facilitated an even electric field distribution but also served as protective shield for the active material, thereby preventing the formation of "dead Zn". Besides, Yu et al. introduced a stainless-steel mesh (SSM) coated with a rapid ion-diffusing Ag–Zn alloy layer as an anode collector (AZ-SSM@Zn)[73]. This alloy layer accelerated Zn^{2+} ion diffusion, regulated flux uniformity, and suppressed HER (Fig. 4f). The AZ-SSM@Zn anode, when matched with commercial activated carbon, exhibited superior rapid charge and discharge capabilities. Even under a high current density of 5A g^{-1} for 4,000 cycles, the capacity retention rate remained close to 100%.

Overall, metal current collectors are endowed with excellent conductivity and mechanical properties, which are pivotal for enhancing the battery cycling performance. The intrinsic zincophilic nature of these metal substrates promotes the uniform deposition of Zn, a critical factor in mitigating dendrite growth and ensuring stable operation. The strategic deployment of single or composite metals, along with the incorporation of alloys, to fabricate 3D anode current collectors is a burgeoning research avenue aimed at stabilizing Zn anodes and augmenting the performance of AZIBs.

3.2.2 *Carbon-based current collectors with a disordered structure*

In general, carbon materials have high conductivity, large specific surface areas, and porous structures, which provide abundant nucleation sites for Zn deposition and optimize surface electric field distribution. These attributes are consistent with the design criteria for 3D Zn anode current collectors[74–76]. Notably, certain unique structures in carbon materials can affect Zn precipitation. For example, graphene, with its atomic arrangements similar to the Zn(002) crystal planes, can be strategically utilized to induce Zn deposition along the (002) plane, thereby promoting uniform deposition and inhibiting dendrite growth[77]. Here, the application of carbon materials in the disordered Zn anode collector as the host was discussed. Carbon nanotubes (CNTs) are lightweight and stable one-dimensional materials, which can be used as a conductive scaffold for Zn anode current collectors, achieving dendrite-free Zn plating/stripping. Zeng et al. demonstrated the importance of a flexible CNT framework as the conductive host for Zn anode current collectors[25]. They adopted chemical vapor deposition to grow CNTs on a carbon cloth (CC), thereby effectively reducing Zn nucleation overpotential and improving the homogeneous electric field distribution (Fig. 5a). The as-fabricated Zn/CNT anode exhibited highly reversible Zn deposition/stripping behavior with a high coulombic efficiency (CE). In a parallel approach, Cao et al. have grown 3D nitrogen-doped vertical graphene nanosheets directly on a CC (N-VG@CC) as a current collector to achieve dendrite-free Zn anodes[81]. This nitrogen-containing group in N-VG remarkably enhanced the Zn affinity of carbon-based current collectors, thereby promoting uniform Zn deposition. In elucidating the underlying mechanism of this Zn affinity, Xie et al. used carbon hollow spheres (referred to as CnC HS), derived from resorcinol formaldehyde, as model current collector[78]. As shown in Fig. 5b, the pyridinic nitrogen sites were attached by Zn^{2+} ions after Zn deposition, leading to the formation of the Zn–N bonds. The establishment of these Zn–N bonds not only altered the chemical state of the initial pyridinic, aligning it with that of graphitic nitrogen, but also promoted Zn nucleation and inhibited Zn dendrite formation.

Constructing 3D carbon nanomaterials doped with heteroatoms is a promising strategy for the development of Zn anode current collectors, as these

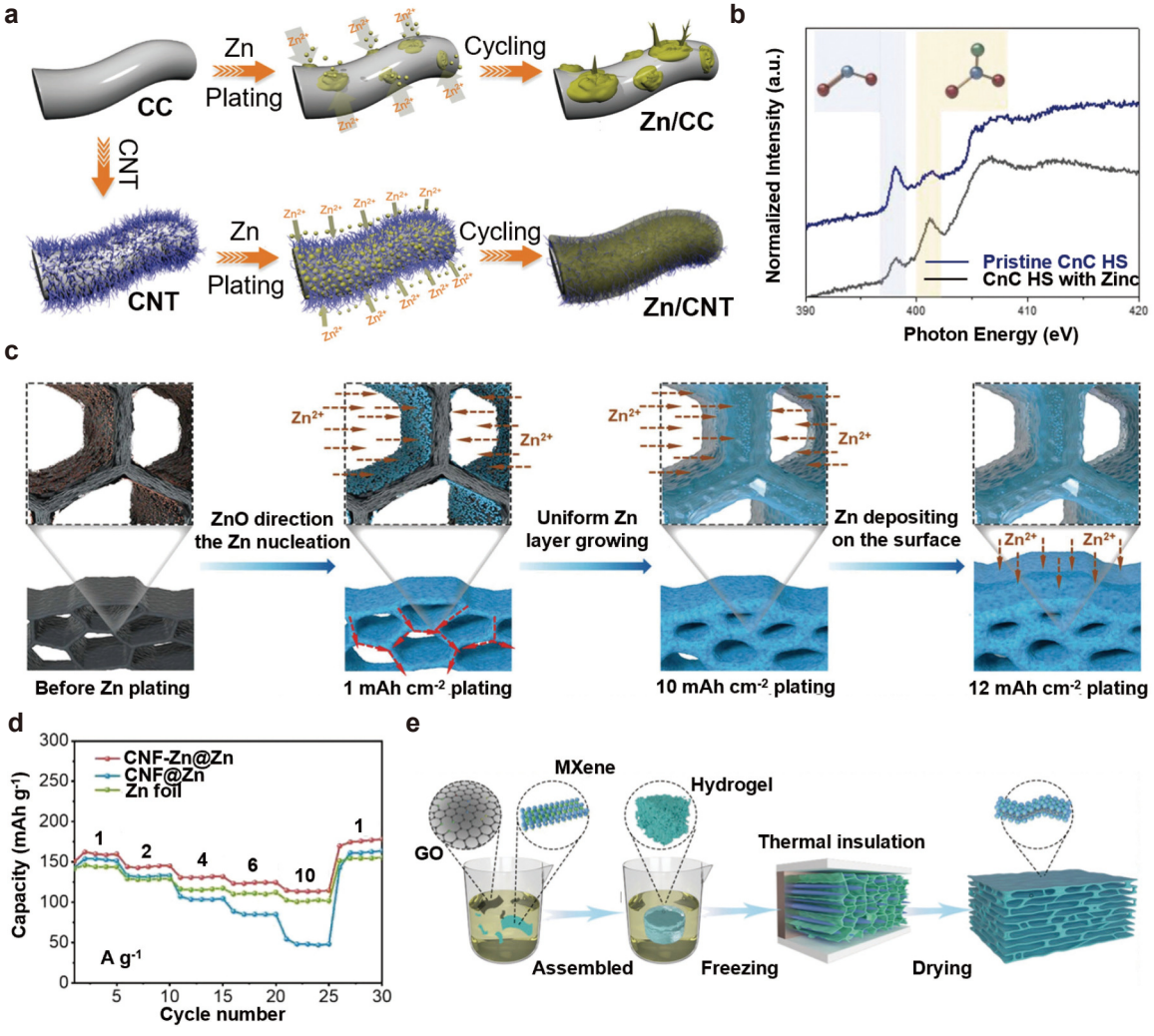

Figure 5 Carbon-based current collectors with a disordered structure. (a) Schematic illustrations of Zn deposition on CC and CNT electrodes. Reproduced from Ref. [25] with permission ©2019, Wiley-VCH Verlag GmbH & Co. KGaA, Weinheim. (b) Nitrogen 1s near-edge X-ray absorption fine structure spectra of pristine CnC HS and CnC HS after Zn deposition. Reproduced from Ref. [78] with permission ©2021, Wiley-VCH GmbH. (c) Schematic illustration of Zn plating on the 3D-ZGC host under various electrochemical conditions. Reproduced from Ref. [21] with permission ©2022, Wiley-VCH GmbH. (d) Rate capabilities of full batteries using the NVO cathode and different anode hosts. Reproduced from Ref. [79] with permission ©2023, American Chemical Society. (e) Schematic illustration of the fabrication process for the MGA material. Reproduced from Ref. [80] with permission ©2021, Wiley-VCH GmbH.

heteroatoms enhance the affinity for Zn deposition. Metal–organic frameworks (MOFs), which are known for their periodic nanoporous structures and exceptional specific surface areas[82,83], yield carbon-derived materials that can function as anode current collectors, effectively suppressing dendrite formation and HER[84]. Xue et al. designed a 3D framework by combining CNTs and graphene into a hierarchical porous structure (3D-ZGC), onto which they introduced MOF-derived ZnO/C nanoparticles[21]. The 3D porous frameworks, in conjunction with ZnO particles that exhibit Zn affinity, induce uniform Zn deposition (Fig. 5c). The symmetric battery using 3D-ZGC as the electrode current collector cycled 1,500 times at a high current density of 20 mA cm^{-2} with a low overpotential of less than 65 mV. Carbon nanofibers (CNF) are also considered viable candidates for Zn anode current collectors. Wang et al. used an eco-friendly strategy to fabricate a flexible 3D CNF architecture with uniformly distributed Zn seeds (CNF-Zn) derived from bacterial cellulose[79]. The CNF-Zn@Zn||$NaV_3O_8{\cdot}1.5H_2O$ (NVO) AZIBs exhibited a remarkably improved rate capability and cycling stability (Fig. 5d). Yu et al. designed a 3D macroporous fiber network current collector, featuring carbon cages decorated with hierarchical lotus root-like Zn/N-doped carbon hollow nanofibers (LRZCF@CC)[85]. The layered 3D hollow network of LRZCF@CC fibers provided additional space to accommodate metallic Zn, effectively addressing volume expansion during cycling.

Apart from the modulation of zincophilic properties, the design of current collectors plays a pivotal role in the formation of the solid electrolyte inter-

phase (SEI) layer. Zhou et al. have constructed an anode collector by integrating MXene sheets onto a flexible reduced graphene oxide framework, utilizing an oriented freezing technique to fabricate an MXene/graphene aerogel structure (Fig. 5e)[80]. The inherent fluorine-terminated surface of MXene contributed to the *in situ* formation of an SEI enriched with Zn fluoride during cycling, which effectively suppressed dendritic growth.

The majority of 3D Zn anode current collectors, which are characterized by their disordered structure and constructed on carbon substrates, have achieved CE exceeding 95%[86]. Heteroatom doping remarkably affects the overall performance. Composite bases, in contrast to single-carbon materials, often exhibit superior performance.

3.2.3 *Other disordered current collectors*

Apart from the abovementioned materials, researchers have also explored alternative materials for the construction of disordered anode collectors. For example, metal/carbon composite materials have been used as composite-based current collectors. Tao et al. reported a leaf-like Zn-coordinated zeolitic imidazolate framework (ZIF-L) nanoflake with atomically dispersed Cu, which is grown onto a Ti mesh (CuZIF-L@TM), serving as the collector (Fig. 6a)[87]. The 3D conductive framework connected by ZIF-L effectively reduced the local current density and homogenized electric field distribution, thereby

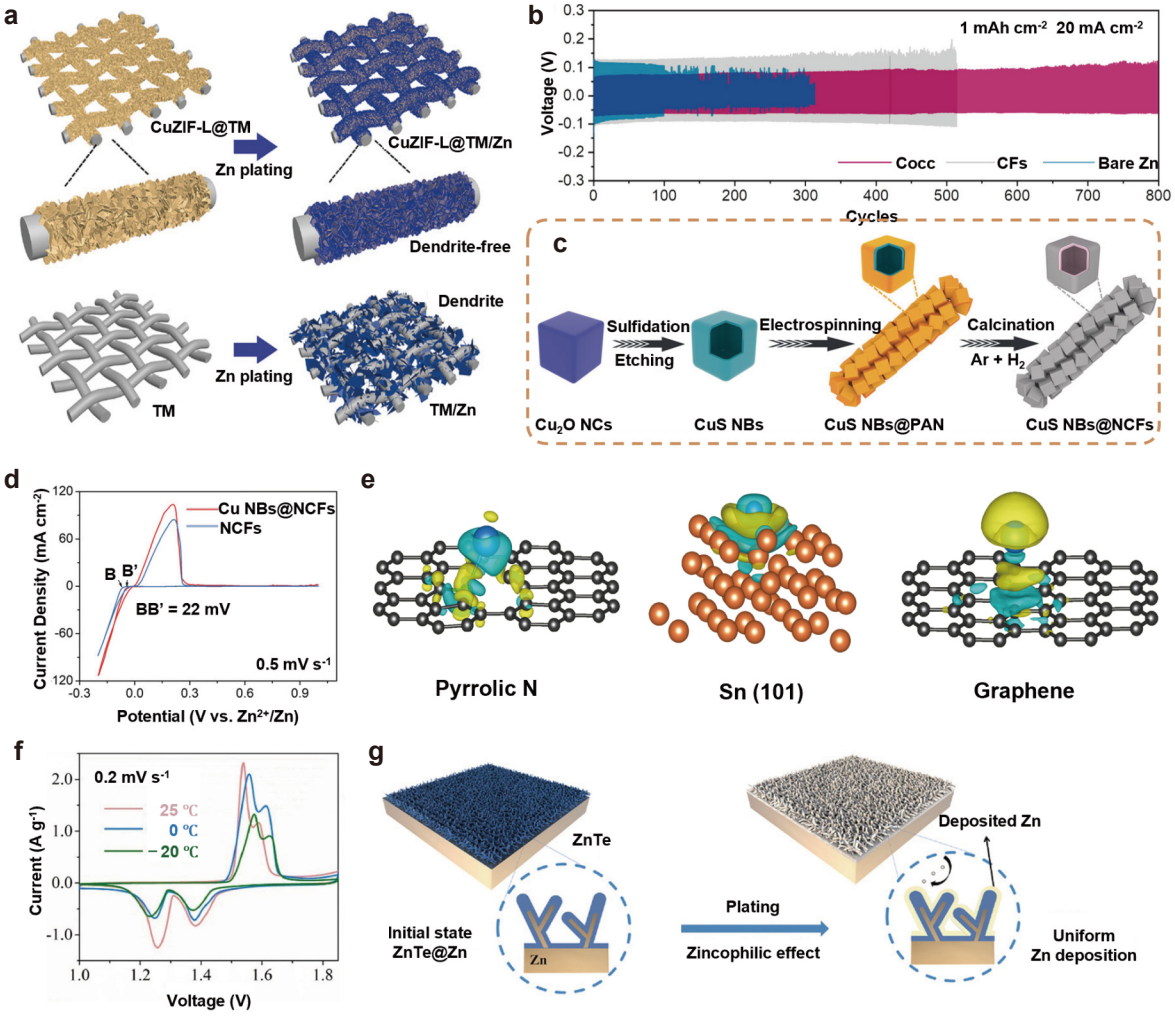

Figure 6 Other disordered current collectors. (a) Schematic illustrations of Zn depositions on CuZIF-L@TM host and TM host. Reproduced from Ref. [87] with permission ©2022, Wiley-VCH GmbH. (b) Long-term cycling performance of symmetric cells under a current density of 20 mA cm^{-2} with a capacity of 1.0 mAh cm^{-2}. Reproduced from Ref. [88] with permission ©2022, American Chemical Society. (c) Schematic illustration of the synthetic procedure for Cu NBs@NCFs. (d) CV curves of the asymmetric cells employing Cu NBs@NCFs and NCF electrodes at a scan rate of 0.5 mV s^{-1}. Reproduced from Ref. [89] with permission ©2022, Wiley-VCH GmbH. (e) Interfacial charge density models for pyrrolic N, Sn(101), and graphene. Reproduced from Ref. [90] under the CC BY-NC 4.0 license ©2022, The Authors. (f) CV curves of wood-based flexible antifreezing AZIBs at various temperatures. Reproduced from Ref. [91] with permission ©2022, Elsevier B.V. (g) Illustrations depicting the Zn plating behavior on the ZnTe@Zn electrode. Reproduced from Ref. [92] with permission ©2022, Wiley-VCH GmbH.

lowering concentration polarization. Meanwhile, Li et al. designed a carbon fiber-based collector host scaffold with zincophilic porous Co-embedded carbon cages (denoted as CoCC)[88]. They implemented a "hierarchical confinement strategy" that maximized the benefits of zinc-binding affinity sites while improving kinetics and stability. This strategy enabled dendrite-free Zn plating/stripping behavior, exhibiting exceptional stability over 800 cycles at a high current density of 20 mA cm^{-2} and a low overpotential of 65 mV (Fig. 6b). In addition, Zeng et al. developed a 3D carbon nanostructure with metal-based zincophilic sites[89]. This 3D multifunctional collector, which is composed of zincophilic Cu nano boxes and N-doped carbon fibers (Cu NBs@NCFs), is illustrated schematically in Fig. 6c. This hierarchical Cu NBs@NCFs host was conductive to Zn deposition along the Zn(002) plane, facilitating smooth Zn plating. Compared with pristine NCFs current collector, Cu NBs@NCFs exhibited superior Zn plating/stripping performance, with reduced polarization and improved reaction kinetics (Fig. 6d). In another study, Yu et al. reported a 3D hybrid fiber directly embedded with N-doped Sn nanoparticles (Sn@NHCF)[90]. The strong Sn–Zn affinity, which is supported by density functional theory simulation results (Fig. 6e), reduced Zn aggregation on the surface and prevented dendrite formation. This robust Zn affinity on the Sn@NHCF substrate during deposition could alleviate Zn aggregation, thereby preventing the formation of Zn dendrites.

Furthermore, various materials have been explored as Zn anode current collectors, such as semiconductor[92] and wood[91]. Wood-based collector was fabricated by ultraviolet light irradiation-assisted delignification of wood veneer, with conductivity derived from nickel and Zn-plated layers. This wooden current collector effectively limited the two-dimensional (2D) diffusion of Zn^{2+} ions, thereby facilitating desolvation, which in turn enhanced Zn deposition kinetics and led to a more homogeneous deposition. As shown in Fig. 6f, the wood-based AZIB with wood@Ni@Zn as the anode and wood@Ni coated with α-MnO_2 as the cathode achieved stable performance even at low temperatures. The resilience of wooden current collectors to deformation and their adaptability to low-temperature conditions indicate their great potential for diverse flexible energy storage applications. For example, the ZnTe semiconductor collector exhibited zincophilic properties that induced Zn deposition along the (002) plane, whereas its excellent mechanical properties withstand the anode volume changes during cycling (Fig. 6g). The architecture of this current collector prevented the formation of Zn dendrites, whereas its high chemical stability mitigated metal corrosion and HER. Thus, semiconductor materials can be incorporated into the design of an anode current collector in AZIB, thereby suppressing the dendritic structure growth.

3.3 Zn powder anodes with a disordered structure

Despite the low cost, controllable particle size, and N/P ratio of Zn powder anodes compared with a Zn foil anode, their practical application has been hindered by inherent limitations. The Zn powder anode is susceptible to corrosion, leading to the formation of surface voids and cracking during static and cycling processes in aqueous electrolytes. This degradation affects the structural integrity of the anode[93]. In addition, Zn electrodes undergo volume changes during charge/discharge cycles. The structural instability of the Zn powder anode exceeds the elasticity limit of the binder, initiating binder failure that propagates from the interior of the material[17]. Although Zn powder anode electrodes exhibit high electrochemical activity, they lack macroscopic electrical conductivity. The stripping of Zn powder leads to volume reduction, thereby causing the loss of physical contact among adjacent Zn powder particles. This loss of electrical contact sharply increases polarization voltage, thereby leading to the rapid failure of the Zn powder anode over a short operational lifespan.

Semi-liquid electrodes provide a solution to the stress concentration issues associated with the rigid structure of conventional solid Zn powder electrodes. Semi-liquid materials are non-Newtonian fluids, which consist of a direct mixture of two-phase substances with specific contents, such as metal particles and liquids[94]. This homogeneous colloidal dispersion exhibits fluidity and liquid-like rheological (shear thinning) properties when subjected to vibration. Under external forces, the semi-liquid material loses its strength to release deposition stress. Therefore, semi-liquid anodes provide dendrite-free plating behavior similar to the function of liquid metals. Zhang et al. designed a semi-liquid anode (SLA) by mixing Zn powder with a dual conductive (ionically and electronically) poly(ethylene glycol) (PEG)-Zn^{2+}/carbon composite matrix (Fig. 7a)[95]. This unique anode utilized its rheological properties to effectively release stresses caused by Zn plating, especially at high current densities. The dual conductive network within the SLA ensured a homogeneous Zn^{2+} flux and facilitated stripping/plating throughout the bulk of the electrode. As shown in Fig. 7b, the SLA endowed the full battery with impressive long-term cycle performance, achieving over 600 cycles with a capacity of 250 mAh g^{-1}. In addition, Sn powder was incorporated as a zincophilic additive within polyacrylamide elastic rheological networks, where Zn was uniformly deposited on dispersed Sn

清華大學出版社 Tsinghua University Press | SciOpen

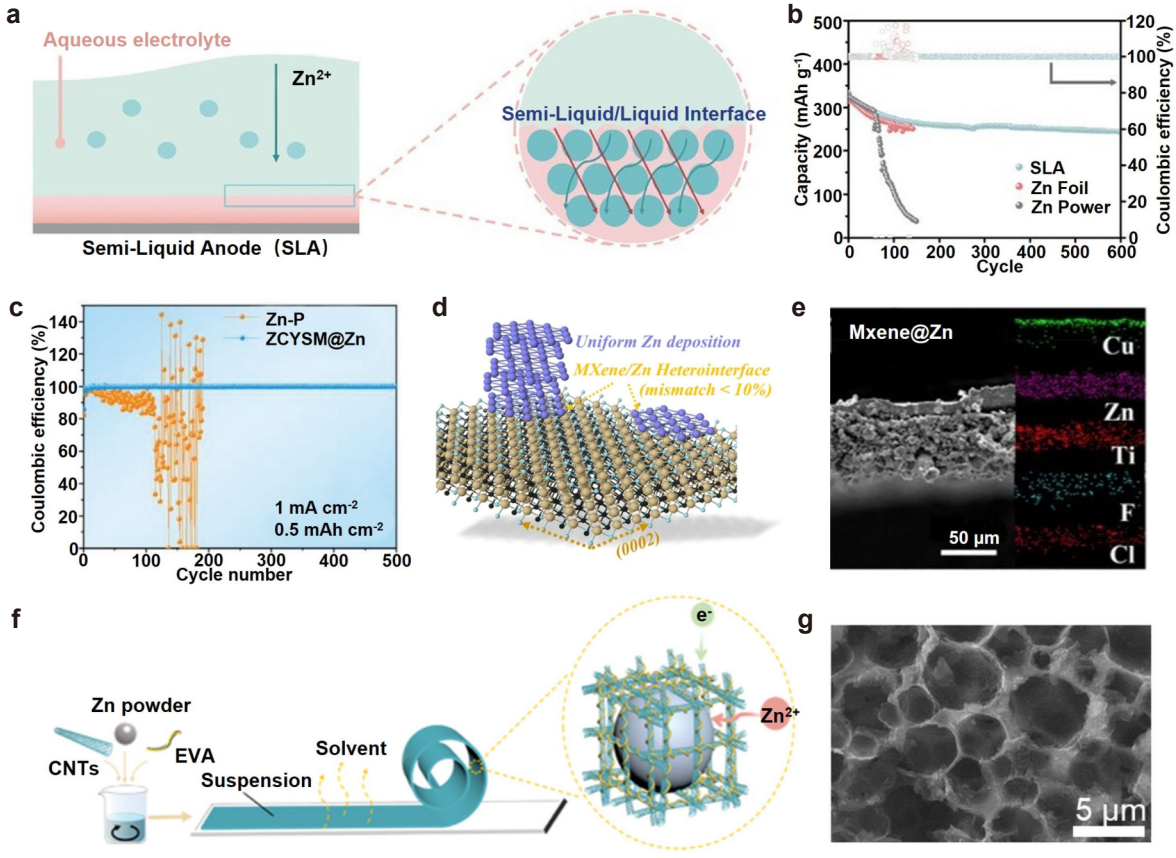

Figure 7 Zn powder anodes with a disordered structure. (a) Schematic illustrations of the morphological evolution of SLA/Zn powder anodes. (b) Cyclic performance of the Zn||$Cu_xV_2O_5{\cdot}nH_2O$ full cell at 1 A g^{-1}. Reproduced from Ref. [95] with permission ©2023, Wiley-VCH GmbH. (c) CE of Zn plating/stripping for the ZCYSM@Zn electrode at 2 mA cm^{-2} with a capacity of 1 mAh cm^{-2}. Reproduced from Ref. [96] with permission ©2023, Wiley-VCH GmbH. (d) Atomic-level illustration of the heterointerface and uniform Zn depositions. (e) Cross-sectional SEM image of the MXene@Zn anode on a Cu substrate, with energy dispersive spectroscopy (EDS) elemental mapping of Cu, Zn, Ti, Cl, and F. Reproduced from Ref. [17] with permission ©2021, American Chemical Society. (f) Schematic illustration of the synthesis procedure for the fabrication of Zn-P-MIEC. Reproduced from Ref. [30] with permission ©2022, Wiley-VCH GmbH. (g) SEM image of the carbon network after Zn etching for the bulk Zn@C composite anode. Reproduced from Ref. [97] with permission ©2024, Wiley-VCH GmbH.

particles, thereby preventing the agglomeration of Zn deposition and mitigating volume changes during repeated Zn stripping/plating cycles[98]. In another report, Li et al. proposed a high-performance soft-solid-phase viscoelastic Zn powder composite anode, utilizing an oligomer gluing strategy. Given its viscoelasticity, the soft-solid Zn powder composite (ss-ZnP) anode remarkably enhanced the charge transfer, weakened the volume effect, and homogenized the interfacial electric field. This phenomenon resulted in fast plating/stripping kinetics and a dendrite-free deposition morphology[99]. Given the low viscosity of the substrate in rheological soft-solid electrodes, conductive fillers were allowed to respond to stresses induced by volume changes, reconstructing conductive paths by diffusion or induced dipole interactions. This reaction effectively mitigated the electrical contact failure in rigid porous structures, effectively extending the cycling life of Zn powder anodes.

The conventional doctor-blade coated Zn powder anode cannot alleviate Zn powder corrosion and electrode delamination during long cycling process. Thus, researchers have endeavored to address these challenges by refining the porous structure of Zn powder electrodes[100–102]. Liu et al. developed porous Zn@C solid hollow yolk–shell microsphere membranes as Zn anode antifluctuation agents. The yolk–shell microsphere (ZCYSM) films exhibited good buffering properties, effectively confining Zn deposition within their structure and inhibiting volume expansion during plating/stripping cycles. Consequently, the ZCYSM@Zn electrode demonstrated a stable and reversible voltage profile for over 4,000 h. The ZCYSM@Zn||Ti cell delivered an ultra-long cycle life of 500 cycles with an average CE of 99.52% (Fig. 7c).

Recently, Niu et al. anchored zincophilic Bi metal nanosheets onto the surface of Zn powder anodes, where zincophilic metals served as preferential Zn

nucleation sites and as charge-aggregated protrusions. The resulting gradient-free Zn^{2+} ion distribution across the powder electrode contributed to an unprecedented life exceeding 5,600 h at a current density of 1 mA cm^{-2}. Furthermore, this innovative approach achieved an exceptionally high Zn utilization of 60% (with 40 mA cm^{-2} and 10 mAh cm^{-2})[103].

The inherent volume expansion associated with Zn powder electrodes poses challenges when paired with planar collectors such as Cu foils, necessitating the development of self-supporting porous structures to enhance 3D ionic and electronic conductivity, thereby homogenizing ion flux. Wu et al. designed a binder-free anode using the spontaneous reaction of commercial Zn powder and graphene oxide[104]. The remaining functional groups on the graphene sheets endowed the electrodes with intact and robust mechanistic properties. A stable, highly reversible, and dendrite-free Zn powder anode was constructed using 2D flexible conducting $Ti_3C_2T_x$ MXene flakes with a hexagonally and closely spaced lattice as a redistributor of electrons and ions[17]. The low lattice mismatch (~10%) led to the formation of a coherent, non-uniform interface between the (0002) side of deposited Zn and the (0002) side of $Ti_3C_2T_x$ MXene (Fig. 7d). This interface induced rapid homogeneous nucleation of Zn^{2+} and sustained reversible stripping/plating with minimal energy barriers through internally bridged shuttle channels. The MXene@Zn anodes were coated on a Cu substrate (Fig. 7e), revealing densely stacked MXene@Zn composite spheres that formed a flat yet rough surface.

Apart from optimizing conductive additives, polymers could also serve as versatile scaffolds for Zn powder electrodes. Liang et al. used ethylene-vinyl acetate (EVA) copolymers as scaffolds, introducing a mixed ionic–electronic conducting scaffold into Zn-P (donated as Zn-P-MIEC) to fabricate flexible and dendrite-free Zn anodes via a scalable tape-casting strategy (Fig. 7f). The high ductility of EVA allowed for easy curling without cracking, and the electrodes maintained their integrity even after repeated folding, demonstrating their excellent flexibility. Recently, Han et al. developed a 3D continuous carbon network-reinforced Zn-powder-based composite anode (Zn@C) by utilizing glucose as a carbon precursor to *in situ* form a carbonaceous layer on the surface of the Zn powder. Subsequently, they used spark plasma sintering to remelt and reconnect the carbon layer into a continuous conductive network (Fig. 7g)[97]. The Zn@C electrode achieved favorable results in suppressing side reactions and improving electrical conductivity, providing valuable insights into industrial-scale fabrication. Similarly, a Zn composite anode was developed by compacting Zn powder with zincophilic site-enriched nanosheets. This anode design effectively fastened ion diffusion and charge transfer kinetics, thereby boosting the fast-cycling performance of AZIBs. The symmetric cell exhibited excellent durability, sustaining for over 13,000 cycles at 50 mA cm^{-2} with 1 mAh cm^{-2}[105].

In general, research on Zn powder electrodes remains in its early stages because of the complex electrochemistry of Zn powder. Further studies should focus on understanding the mass transport and charge transport mechanisms of Zn powder electrodes. Ensuring the structural integrity and electrochemical performance of the porous structure during extensive cycling remains a critical area for future investigation.

4 Porous Zn anodes with an ordered structure

In general, porous Zn electrodes exhibit macroscopic isotropy, incorporating active materials, conductive additives, binders, and an interconnected network of pores. However, the tortuous nature of ion migration within these pores, coupled with the anisotropic electric field during battery operation, leads to non-uniform mass transport along the direction of the electrode depth[106]. This phenomenon results in a concentration gradient that causes disparate reaction kinetics at varying depths, with not all active materials being accessed and activated simultaneously[107,108]. The difference in charge transport kinetics and reaction kinetics results in the polarization and insufficient utilization of active materials, especially at high current rates. Under certain magnification conditions, the reaction polarization increases with the electrode thickness because of the prolongation of the diffusion path[109]. The preferential deposition of Zn^{2+} ions at regions of higher ion flux, such as the separator–anode interface, can induce "top growth" and Zn dendrite formation. Therefore, designing electrodes with tailored structures is important to regulate charge transfer. In particular, the development of electrodes with gradient microstructures or compositions along the depth direction can reduce the resistance of the process during charge transfer, thereby compensating for the reactive polarization. By controlling the surface zincophilicity or conductivity of the electrode framework, the diffusion and deposition dynamics of Zn^{2+} ions can be regulated, thereby improving the rate performance and power density of AZIBs.

4.1 Zn foil anodes with an ordered structure

In general, most of the porous structures constructed on the surface of Zn foils are created using etching agents. However, the deployment of these agents necessitates meticulous control over their concentra-

清華大學出版社 Tsinghua University Press | SciOpen

tion and the duration of etching to ensure a uniform array of pores or stripes. Precision is critical to prevent over-etching, which can lead to side reactions at the enlarged active sites. Furthermore, the impact of the resultant disordered pore structure on the transport path of Zn^{2+} ions and the associated charge transfer resistance has not been extensively investigated. Therefore, designing an ordered structure along the electrode thickness direction is necessary to optimize pore morphology, electrical conductivity, and zincophilicity.

The imprint-induced microchannels, which exhibit enhanced Zn^{2+} affinity, effectively regulate the concentration distribution of Zn^{2+} ion and prevent the risk of short circuits caused by vertical dendrite growth[110]. Utilizing zincophilic Zn foils as the anode (obtained by an *in situ* substitution reaction with Sn salts) improved the deposition behavior at the top of conventionally imprinted electrodes (Fig. 8a). Notably, the microchannel portion of the imprinted electrode displayed a higher concentration of Zn^{2+} ions, directing the preferential migration of Zn^{2+} ions to the inner wall of the microchannel. This redistribution of Zn^{2+} concentration promoted the nucle-

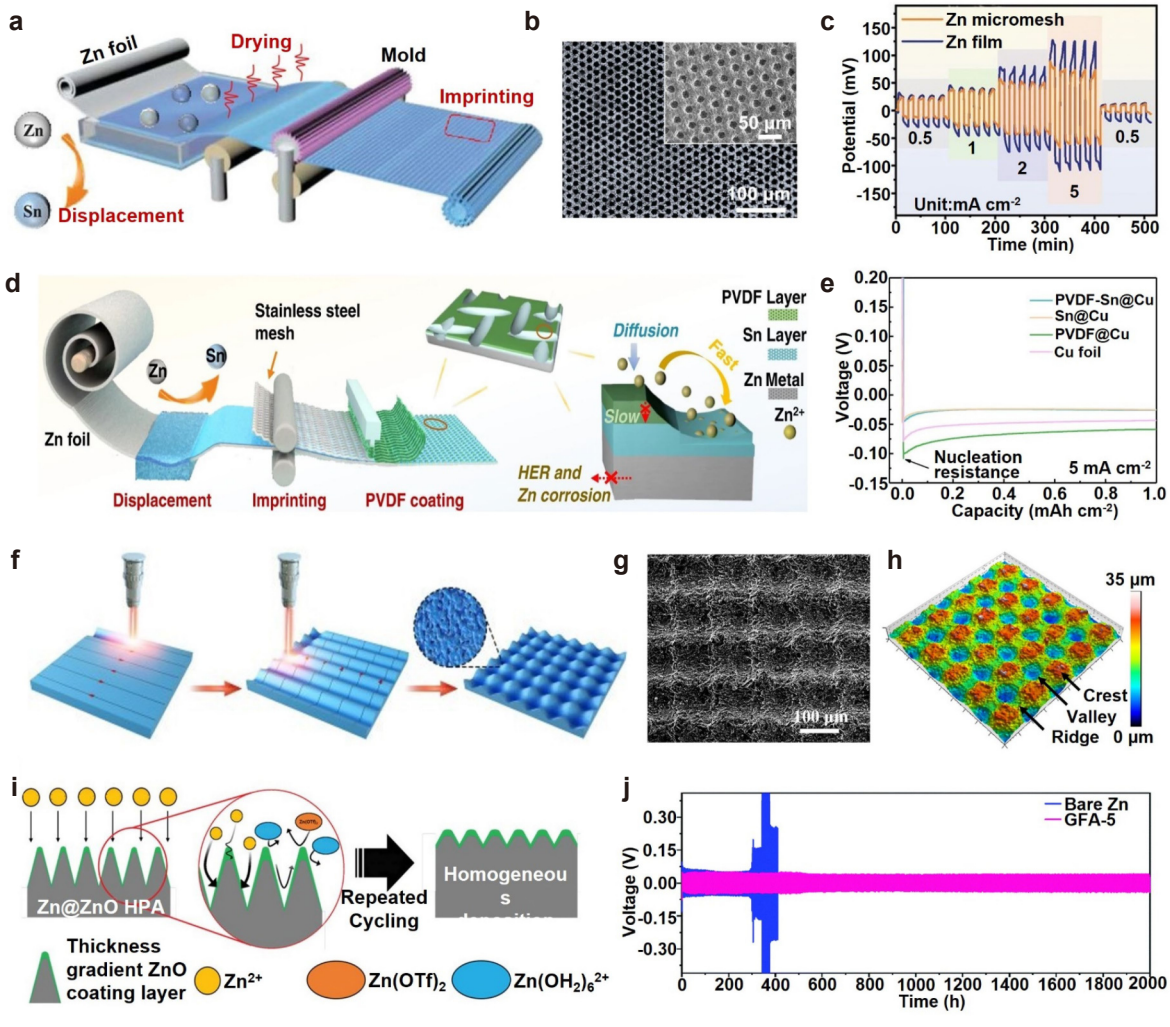

Figure 8 Zn foil anodes with an ordered structure. (a) Schematic illustration of the scalable imprinting technique used for the fabrication of porous Zn anodes. Reproduced from Ref. [110] with permission ©2022, Wiley-VCH GmbH. (b) Microscopic photo of a Zn micromesh, with an inset showing a SEM image of the Zn micromesh. (c) Rate performance of the symmetric cells based on Zn micromesh and Zn film anodes at current densities ranging from 0.5 to 5 mA cm^{-2}. Reproduced from Ref. [28] with permission ©2021, Wiley-VCH GmbH. (d) Schematic illustration of the fabrication of a PVDF-Sn@Zn gradient electrode and the subsequently induced Zn deposition. (e) Voltage–time curves for Zn deposition at a constant current density of 5 mA cm^{-2} on different electrodes. Reproduced from Ref. [20] under the CC BY 4.0 license ©2023, The Authors. (f) Schematic depiction of the top-down fabrication of the geometrically periodic concave-convex laser lithography-patterned Zn foils (LLP@ZF) by nanosecond laser lithography. Low-magnification SEM image (g) and confocal light microscope map (h) for the surface morphology of LLP@ZF. Reproduced from Ref. [111] with permission ©2022, Elsevier B.V. (i) Schematic illustration of the deposition behavior of Zn ions on the Zn@ZnO HPA anode in an aqueous electrolyte. Reproduced from Ref. [27] with permission ©2020, Wiley-VCH Verlag GmbH & Co. KGaA, Weinheim. (j) Voltage profiles of the modified Zn anode at a current density of 1 mA cm^{-2} and a capacity of 1 mAh cm^{-2}. Reproduced from Ref. [112] with permission ©2022, The Royal Society of Chemistry.

ation and deposition of Zn^{2+} ions at the inner wall of the microchannel, thereby preventing uneven deposition and dendrite growth[113]. The majority of reported structurally engineered Zn anodes have not achieved precise control over the actual dimensions of the 3D network and efficient regulation of the micro/nanostructure, thereby failing to utilize the full potential of the porous design[114]. In particular, cross-scale variations and the disordered nature of micro/nanopores decreased the charge transport rate[115]. By contrast, electrodes with regularly arranged structures show superior performance over their disordered counterparts by achieving highly organized charge transfer pathways and adjustable internal voids. Zhang et al. synthesized flexible, ultrathin, and ultralight Zn micromesh (with a thickness of 8 μm and an areal density of 4.9 mg cm^{-2}) through a synergistic approach combining photolithography and electrochemical processing, resulting in the regular arrangement of micropores[28]. The engineered microporous Zn micromesh exhibited excellent flexibility, enhanced mechanical strength, and improved wettability (Fig. 8b). The voltage hysteresis of Zn micromesh symmetric cells was consistently lower than that of cells assembled with Zn films across all tested current densities. This difference became more pronounced with the increase of current density (Fig. 8c). Guan et al. reported an imprinted gradient Zn anode (PVDF-Sn@Zn) that integrated conductive and hydrophilic gradients[20]. The top layer, which is composed of hydrophobic and insulating PVDF, and the bottom layer, which consisted of hydrophilic and conductive Sn, worked synergistically to enhance the corrosion resistance of the Zn anode and inhibited the HER (Fig. 8d). This bottom-up deposition behavior of Zn metal could effectively avoid the issue of top dendrite growth. As shown in Fig. 8e, the PVDF-Sn@Cu gradient electrode demonstrated the lowest nucleation overpotential (18.9 mV), indicating that the optimized gradient structure facilitated Zn nucleation and deposition. The well-designed regular pore structure fully exploited the ability of micropores to induce a favorable ion concentration and current distribution, a phenomenon that can be rationalized through computational simulations.

Laser-based techniques can precisely control the arrangement and size of micropores on the surface layer of Zn foils, thereby modulating Zn deposition and enhancing electrochemical performance. Yang et al. applied laser processing to create a periodic concave–convex pattern on commercial Zn foils (Fig. 8f)[111], resulting in hydrophilic properties caused by enhanced wettability. This uniform secondary roughness, combining microscale and nanoscale features, was attributed to localized Zn melting and evaporation during lasering. The periodic patterned egg crate-shaped concave–convex surface is shown in Fig. 8g. The confocal light microscope map confirmed well-defined crests (red), ridges (green), and valleys (blue), with consistent intervals and height differences (Fig. 8h). Laser processing also enabled vertical gradient conductivity in Zn electrodes, as demonstrated by Huang et al. who developed a gradient Zn anode with an insulating hydrophobic passivation layer at the top and a conductive hydrophilic fresh Zn layer at the bottom[18]. This design effectively reduced corrosion and guided Zn deposition to prevent dendrite growth.

The construction of gradient porous structures on the surface of Zn foils often requires novel fabrication processes and sophisticated designs. As illustrated in Fig. 8i, Lee et al. engineered a novel Zn metal electrode with a compositionally and morphologically controllable surface through periodic anodic oxidation, resulting in a ZnO layer with a gradient thickness coated on a Zn hexagonal pyramidal array (Zn@ZnO HPA)[27]. The ZnO islands, formed through homogeneous dissolution and selective deposition, exhibited a thickness gradient that diminished from the top to the bottom (Fig. 8i). The ZnO coated on hexagonal pyramidal structures induced Zn^{2+} ion plating at the sides and bottom because of their relatively low interfacial resistance and served as passivation layers against aqueous electrolytes. Zhi et al. have introduced a simple *in situ* constructed porous framework coating that not only eliminated Zn dendrites but also suppressed HER[112]. This coating consisted of spatially gradient fluorinated alloy (GFA) nanoparticles, with ZnF_2 in the outermost layer and CuZn alloy in the inner layer. The lateral growth within the GFA coating was induced by the formation of CuZn alloys within the particles, which stored the plated Zn and filled the interparticle voids, thereby adapting to a dendrite-free morphology. Consequently, the symmetric cell demonstrated excellent long-term cycling stability over 2,000 h (1,000 cycles) with stable voltage profiles at 1 mA cm^{-2} and 1 mAh cm^{-2} (Fig. 8j). Despite these advancements, a cohesive theoretical framework elucidating the impact of pore structures on the electrochemical kinetics of Zn anodes in AZIBs remains unknown, which requires further investigation and development.

4.2 Current collectors with an ordered structure

Designing 3D porous current collectors is a prevalent approach to address the challenges associated with Zn electrodes. The enhanced specific surface area of these current collectors reduces the localized current density at the 3D Zn electrode, thereby decreasing the overpotential and moderating Zn deposition. Carbon-based materials, which are known for their high electrical conductivity, light

清華大學出版社 Tsinghua University Press | SciOpen

weight, and facile fabrication, are commonly used as conductive substrates for Zn anodes.

However, the uneven ion flux distribution at high current densities leads to Zn deposition on the upper surfaces of the porous structures, resulting in the inefficient utilization of 3D space and potentially causing short-circuit issues due to dendrite growth. Therefore, strategically manipulating the electric field distribution and ion concentration by rationally designing a spatial structure of the carbon-based current collectors is of great importance. Zhao et al. developed two 3D hierarchical graphene matrices consisting of nitrogen-doped graphene nanofiber clusters (GFs) anchored on vertical graphene arrays (VGs) of modified multichannel carbon (Fig. 9a)[32]. The Zn metal was deposited along the longitudinal direction (3D-LFGC) and radial direction (3D-RFGC) of the 3D multichannel carbon matrices. The modified carbon matrix exhibited channels with sizes ranging from 10 to 30 μm (with a typical size of 20 μm). In particular, GFs with a diameter of 250 nm and VGs were firmly embedded within the channels, creating a 3D interconnected and versatile framework (Fig. 9b). Compared with 3D-LFGC, 3D-RFGC showed reduced plateau overpotentials at different current densities, indicating lower local current densities and more homogeneous Zn^{2+} ion distributions. This finding was attributed to the effective electrolyte infiltration into the substrate and the robust interaction between Zn and VGs and GFs, which promoted homogeneous Zn ion flux distribution and dense Zn deposition. Apart from modifying ordered graphene arrays, constructing highly organized carbon frameworks to homogenize the ion flux is also a viable approach. Lou et al. developed a highly ordered TiO_x/Zn/N-doped carbon inverse opal (denoted as TZNC IO) to spatially stabilize Zn anodes[116]. The fabrication of TZNC IO involved evaporation-induced self-assembly, impregnation, and calcination (Figs. 9c and 9d). The 3D macroporous framework with a periodic structure allowed precise electric field control, minimizing the local current and inducing uniform Zn deposition. In addition, the interconnected pores provide ample void space to regulate Zn^{2+} ion flux and alleviate volume expansion.

Given the inherent lack of a host for Zn, Zn^{2+} ions nucleate preferentially at defect sites such as dislocations, leading to the formation of dendrite protrusions. To modulate the deposition/stripping behavior of Zn, the design of metal-based current collectors is meticulously optimized to enhance crystal surface orientation, local conductivity, and atomic binding energy, while also engineering orderly pore architectures. The $Zn_{88}Al_{12}$ alloy formed by casting, featured symbiotic Zn and Al lamellas[26], exhibited improved oxidation resistance in air and aqueous electrolytes compared with monometallic Zn because of the formation of a stable and passive Al_2O_3 surface layer that prevented further oxidation (Fig. 9e). The insulating Al_2O_3 shell, which substantially blocked the electron transfer from Al to Zn^{2+}, facilitated uniform Zn deposition at the interlayer spacing along the Zn precursor sites. Compared with the $Zn||K_xMnO_2$ cell, the $Zn_{88}Al_{12}||K_xMnO_2$ cell demonstrated a marked increase in current density, with $Zn_{88}Al_{12}$ showing more reversible deposition/stripping behavior than pure Zn (Fig. 9f). In addition, commercial Cu foams generally suffer from irrational pore distribution and poor utilization of internal space. Jiang et al. developed Cu current collectors with periodically arranged 3D hemispherical pits through a synergistic approach involving photolithography and wet chemistry[117]. The battery based on faceted Cu hemispherical electrodes exhibited a lower charge transfer resistance (18 Ω) than that of pristine Cu electrodes (30 Ω) because of the improved electrolyte wettability (Fig. 9g). The integration of a controllable spatial arrangement with a zincophilic design in porous metal current collectors is emerging as a research trend for dendrite-free AZIBs. However, the complexity and high cost of such batteries hinder their widespread applications.

The application of 3D printing technology as a high-precision additive manufacturing method for energy storage devices has received considerable attention[118,119]. This advanced technique diverges from conventional porous collectors (e.g., Cu foam and CC) by enabling the precise engineering of pore architectures that facilitate controlled ion flux and electric field distribution. Duan et al. innovated a strategy that combined 3D printing with chemical deposition to fabricate conductive 3D nickel lattice current collectors[115]. The process involved the sequential application of chemical and electrochemical deposition to coat a pre-printed 3D polymer framework with a metallic Ni layer, which exhibited strong binding affinity to Zn atoms. Subsequently, the formed conductive metal network was electrodeposited with Zn to yield the final electrodes (Fig. 9h). The multichannel lattice structure of the 3D porous Ni–Zn anode optimized the electric field distribution across the electrode, thereby promoting uniform Zn deposition and enhancing the electrochemical performance of AZIBs. The 3D printing paradigm provides a versatile and customizable platform, with demonstrated efficacy in incorporating advanced materials such as graphene[120] and N-doped interfaces[121] into the fabrication of Zn anodes.

Ion diffusion within the porous electrode plays a key role in the charge transport kinetics; thus, the modulation of the pore structure of electrodes is a strategic approach to regulate ion flux and alleviate polarization. Researchers have used porous carbon

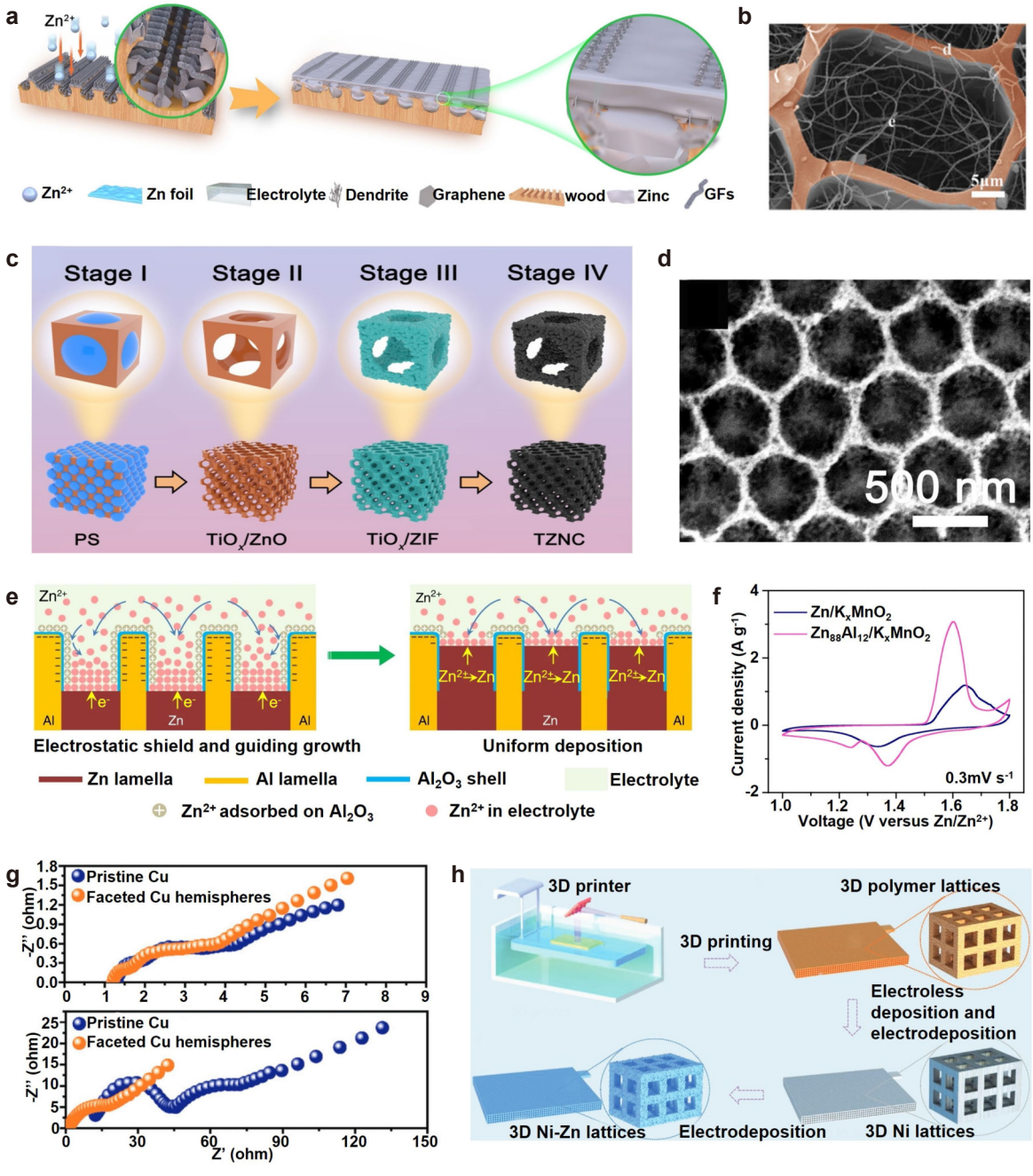

Figure 9 Current collectors with an ordered structure. (a) Schematic depiction of the engineered 3D hierarchical graphene matrix architecture that is designed to stabilize Zn anodes. (b) SEM images of the 3D hierarchical graphene matrix. Reproduced from Ref. [32] under the CC BY 4.0 license ©2023, The Authors. (c) Schematic illustration of the synthesis process for the TiO_x/Zn/N-doped carbon inverse opal (TZNC IO) anode. (d) Field-emission scanning electron microscopic images of TZNC IO. Reproduced from Ref. [116] with permission ©2021, Wiley-VCH GmbH. (e) Schematic illustration of the eutectic strategy utilizing Zn/Al lamellar eutectic structures for suppressing dendrite growth and crack formation. (f) Typical CV curves of $Zn_{88}Al_{12}||K_xMnO_2$ and $Zn||K_xMnO_2$ full cells using eutectic $Zn_{88}Al_{12}$ alloy ($\lambda \approx 450$ nm) or the monometallic Zn as the anode. Reproduced from Ref. [26] under the CC BY 4.0 license ©2020, The Authors. (g) Nyquist plots before and after galvanostatic discharge and charge processes. Reproduced from Ref. [117] with permission ©2023, Wiley-VCH GmbH. (h) Schematic illustration of the fabrication procedure for 3D Ni–Zn lattice structures. Reproduced from Ref. [115] with permission ©2021, Wiley-VCH GmbH.

skeletons or metal structures as the host framework to build 3D structures that facilitate extensive ion diffusion. Despite these efforts, the concentration gradient within the porous Zn anode still induces nonhomogeneous transport of Zn^{2+} ions, which is particularly pronounced in thick electrodes subjected to fast charging and discharging cycles. Zn^{2+} ions are preferentially deposited at the electrolyte–electrode interface, where the ion flux is elevated, rather than within the electrode. This behavior leads to the inefficient utilization of the internal electrode space and the formation of dendrites, which compromises

battery safety and longevity[122,123]. Therefore, designing electrode structures with a pore structure gradient that promotes ion flow toward the interior of the electrode is instrumental in promoting favorable reaction kinetics. Studies have demonstrated that optimizing the electrode porosity through model-based simulations effectively reduces ohmic resistance and increases LIB capacity[124,125]. Given these findings, researchers have implemented gradient porosity in porous Zn anodes for AZIBs, thereby enhancing the overall battery performance[31,126].

Considering that Zn deposition occurs where Zn ions encounter electrons, the electric field distribution plays an important role in regulating Zn deposition. Therefore, constructing a gradient framework that enhances the electronic conductivity from the separator side to the cell shell side is recommended. This design facilitates the directional deposition of Zn from the bottom and grows upward. Several studies have demonstrated the successful implementation of gradient conductivity in porous Zn anodes. By constructing an electronically insulating layer such as Al_2O_3[26], NiO[31,127], or PVDF[110], on top of the electrode structure, a vertical variation in localized conductivity has been achieved. This strategy has been instrumental in achieving dendrite-free AZIBs.

A zincophilic gradient could be constructed in the opposite direction of the Zn ion concentration gradient to regulate Zn ion fluxes within the pore structure. This strategy can be accomplished by incorporating zincophilic metal layers or nanoparticles at the bottom of the electrode, which reduces the nucleation overpotential of Zn ions and increases the ion flux. By meticulously adjusting the thickness, particle concentration, or composition of these zincophilic modifications, a gradient in zincophilicity can be engineered, thereby facilitating a more controlled and efficient Zn deposition[128].

In enhancing the electrochemical performance of AZIBs, studies have explored the integration of zincophilic and conductive gradients into a dual-gradient framework to improve the reaction kinetics by synergistically modulating the ion and electron transport kinetics. In addressing "top growth" associated with commercial Cu foam, Hong et al. fabricated porous foam electrodes with a gradient in conductivity and zincophilicity[127]. As shown in Fig. 10a, a hydrophilic yet electrically insulating NiO layer was formed on the separator side of the electrode by using a novel bilateral template method, complemented by a conductive Cu foam on the cell shell side (Fig. 10b), which exhibited a high binding energy to Zn. This layered deposition strategy achieved a "bottom-to-up" deposition mode, thereby enhancing the capacity and rate performance of the battery. Similarly, a GFA electrode, featuring a conductive bottom layer and an insulating top layer, demonstrated highly reversible Zn plating/stripping behavior for 700 h at 3 mA cm^{-2}[112]. Guan et al. designed a tri-gradient dendrite-free electrode that integrated gradients in conductivity, zincophilicity, and porosity[31]. This tri-gradient design introduced an enhanced Zn^{2+} ion flux and optimized local charge transport kinetics at the bottom of the electrode, facilitating the downward migration of Zn^{2+} ions and promoting the bottom-up deposition of Zn metal (Fig. 10c). Recently, a novel electron/ion flux dual-gradient 3D porous Zn anode has been engineered by using a layer-by-layer bottom-up approach with attenuating Ag nanoparticles (3DP-BU@Zn). This established hierarchical porous architecture facilitated a preferential bottom-up Zn deposition, thereby enhancing the overall anode performance (Fig. 10d)[41]. At a high current density of 5 mA cm^{-2} and a capacity of 2.5 mAh cm^{-2}, 3DP-BU@Zn exhibited low-voltage hysteresis of 41.9 mV within 450 h, surpassing the performance of electrodes without dual-gradient and inverse-gradient designs (Fig. 10e).

4.3 Zn powder anodes with an ordered structure

Given its malleability, Zn powder can be used to fabricate regular porous electrodes through 3D printing[22]. However, the inherent drawbacks of Zn powder anodes, such as susceptibility to corrosion and uncontrolled dendrite growth, have limited their broader applications. Studies have shown that encapsulating the Zn–P surface with 2D conductive materials, such as MXenes, could mitigate volume expansion and dendrite growth. Xu et al. utilized an innovative 3D cold-trap environment printing (3DCEP) technique, which combined laminar flow and ice crystal sensing, to achieve an orderly arrangement of MXene nanosheets during 3D printing[129]. The high lattice matching between MXene and Zn, along with spatial constraints at the MXene interface, inhibited the dendrite growth (Fig. 11a). To solve the issue of uneven MXene encapsulation on Zn powder, which is common in traditional ink direct writing, Pang et al. introduced a novel microfluidic-assisted 3D printing strategy[130]. This strategy used a magneto-thermal flow microfluidic technique that modified the raw materials within the microfluidic channel by external conditions during the ink flow process, inducing the aggregation of MOF and MXene on the surface of Zn powder. The MXene in this context was endowed with a functional layer of Cu-tetrahydroxy-1,4-benzoquinone (Cu-THBQ)-conductive MOF, which provided stable adsorption and diffusion coefficients for Zn^{2+}, facilitating uniform Zn deposition.

Achieving a balance between the design of 3D structures and corrosion mitigation is challenging, as the increased contact area between the electrode and electrolyte exacerbates electrode corrosion[64,132,133]. Consequently, designing appropriate coatings on

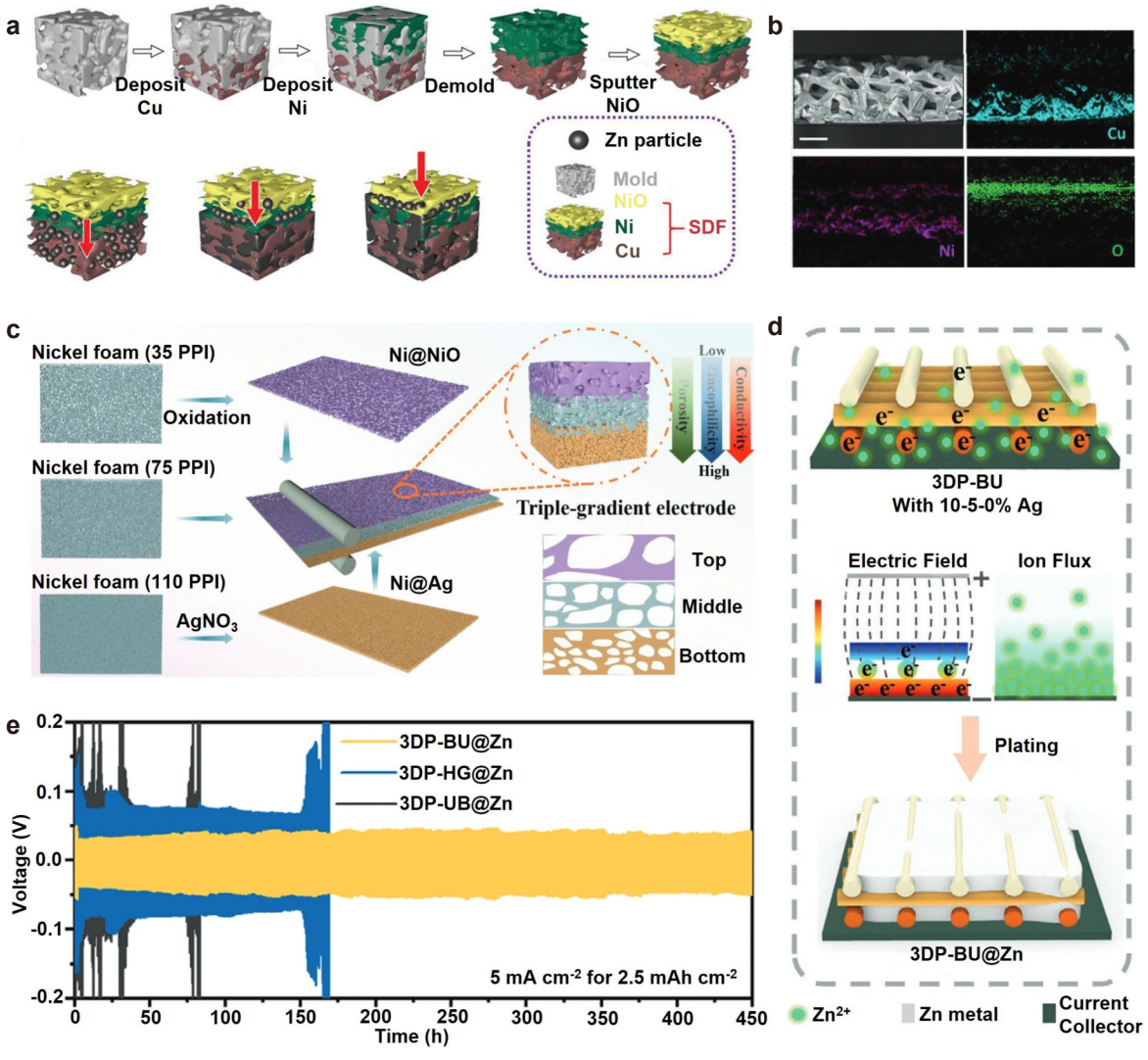

Figure 10 Gradient design of porous current collectors. (a) The prepared procedures of the innovative tri-layers frame collector (SDF) structure. (b) Cross-sectional SEM images of vacant SDF structure with EDS images of Cu, Ni, and O. Reproduced from Ref. [127] with permission ©2021, Wiley-VCH GmbH. (c) Schematic diagram of the triple-gradient electrode fabrication utilizing a mechanical rolling technique. Reproduced from Ref. [31] with permission ©2023, Wiley-VCH GmbH. (d) Schematic diagrams of electron/ion flux dual-gradient scaffolds illustrating the Zn deposition behavior under various electron/ion flux conditions. (e) Cycling performances of different symmetrical cells under a current density of 5 mA cm^{-2} and an areal capacity of 2.5 mAh cm^{-2}. Reproduced from Ref. [41] under the CC BY-NC 4.0 license ©2023, The Authors.

porous Zn anode surfaces is a promising strategy[134,135]. Guan et al. coated a 3D-printed Zn scaffold with a layer of ion-conducting conformal hydrogel composed of sodium alginate and polyacrylamide, demonstrating impressive cycling stability of 4,700 h at 5 mA cm^{-2} and 5 mAh cm^{-2} for the symmetric cell[131]. As illustrated in Fig. 11c, the diffusion behavior of Zn^{2+} during Zn stripping/deposition was modulated by aryl and carboxylate salts within the hydrogel chains, providing specific ion diffusion channels and accelerating Zn^{2+} desolvation, thereby preventing unwanted dendrite growth. Dynamic adaptive hydrogel coatings alleviated stress accumulation from dendrite growth during cycling, maintaining long-term cycling stability of the anode (Fig. 11d).

Furthermore, the same group has pioneered the gradient design strategy for Zn powder anodes, which effectively regulated the Zn deposition behavior[126]. The particle size of the Zn powder and the porosity of the electrodes decreased in the depth direction, generating a bottom-up gradient of ion fluxes along the pore depth (Fig. 11e), which prevented the notorious "top growth" and relieved the stress concentration. Despite these advantages, Zn powder electrodes remain in the nascent stages of exploration, with cycling performance and thick electrode performance yet to meet expectations. The challenge lies in reconciling severe corrosion and structural collapse with the uniform ion fluxes caused by the expanded specific surface area of the porous structure of Zn powder.

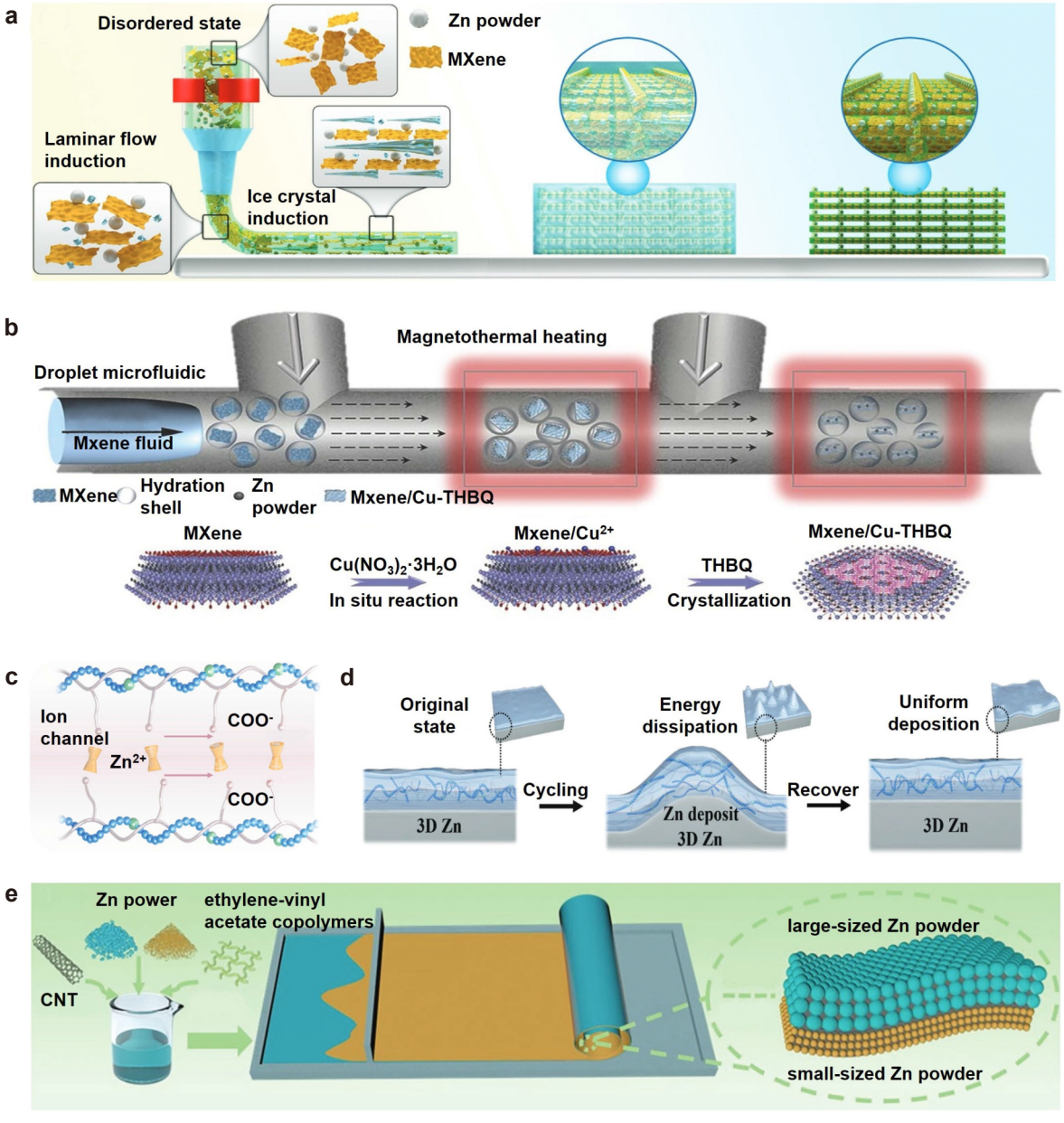

Figure 11 (a) Schematic illustration of 3D cold-trap environment printing for fabricating and aligning MXene/Zn-P aerogel. Reproduced from Ref. [129] with permission ©2023, Wiley-VCH GmbH. (b) Illustration of the microfluidic synthesis of MXene/Cu-tetrahydroxy-1,4-benzoquinone (THBQ)/Zn-P printable mixed ink and the synthetic mechanism underlying the formation of hetero-structured MXene/Cu-THBQ. Reproduced from Ref. [130] with permission ©2023, Wiley-VCH GmbH. (c) Schematic illustration of the ionic diffusion of Zn^{2+} in the hydrogel coating layer. (d) Schematic depiction of the interface coating and protective mechanism provided by a hydrogel layer on porous Zn anodes. Reproduced from Ref. [131] with permission ©2023, Wiley-VCH GmbH. (e) Schematic illustration of the fabrication of the gradient electrode. Reproduced from Ref. [126] with permission ©2023, Wiley-VCH GmbH.

Overall, the meticulously engineered porous architecture (characterized by optimized pore size, orderly pore arrangement, and gradient design), confers remarkable advancements to Zn anodes with regard to electric field distribution, ion flux dynamics, and nucleation overpotential. However, the introduction of a large number of inert materials could reduce the overall energy density of the battery, and the structural stability of these configurations under external stresses must be further investigated.

5 Summary and outlook

AZIBs are emerging as potential energy storage devices because of their inherent safety, low cost, and environmental benignity. However, their commercialization is hindered by challenges, such as persistent side reactions, low CE, and limited DOD for Zn anodes. The adoption of porous structures is a strategic solution to these issues. In this review, the research advancements in the design strategies of porous structures for Zn metal anodes were summa-

rized. Categorizing into disordered and ordered porous anode structures, the relationship between the fabrication method and the pore morphology has been elucidated. We focus on zincophilic modifications and gradient design in porous structure engineering and provide a comprehensive overview of the research on Zn powder anodes. Although remarkable progress has been achieved in recent years, scientific and engineering challenges remain to be addressed for the advancement of porous Zn metal anodes. Therefore, carrying out the following research directions is necessary to design and optimize porous Zn anodes:

1. Material synthesis and structural optimization. The use of porous structures has been instrumental in facilitating uniform Zn nucleation and growth, but it does not inherently prevent the side reactions that arise from the increased surface area. In addition, the fabrication of thick electrodes with low tortuosity provides unique advantages with regard to transport kinetics, a feature that has not been extensively reported in AZIBs. The precise control of low tortuosity electrode structures and the interplay between microstructural characteristics and performances warrant meticulous investigation to promote practical applications of AZIBs. Furthermore, the optimization of preparation methods, the exploration of new template materials, and the improvement of electrochemical corrosion methods are urgently necessary to achieve higher porosity and better structural control in the preparation of porous Zn metal anodes. For example, the use of nanoscale porous structures can enhance reactivity and reduce stress caused by electrode volume changes. The development of porous electrodes with gradient conductivity and zincophilicity is conducive to improving charge transfer kinetics.

Moreover, novel Zn alloy materials should be developed to improve the durability of porous Zn anodes by adjusting the alloy composition and the proportion of different metal elements. Optimizing the grain size and orientation of the alloy anode can further improve ion diffusion and electron conduction. By introducing interface modification layers or coatings, the compatibility and stability between the electrodes and the electrolyte can be enhanced, thereby suppressing electrolyte evaporation and solvent decomposition.

2. Theoretical computation and advanced characterization. Although the development of AZIBs has been of interest in recent years, the theoretical study of the electrochemical kinetics of AZIBs, particularly porous Zn anodes, has remained largely overlooked. Moreover, the applicability of formulas derived from LIBs to AZIBs is yet to be established. Theoretical computations complement experimental findings by exploring physical processes such as reaction kinetics, charge transport kinetics, and structural evolution that extend beyond the limitations of experimental results. The integration of cutting-edge theoretical advancements with precise experimental data modeling is crucial for elucidating the intricacies of reaction kinetics and reversibility of porous Zn anodes.

Meanwhile, a profound understanding of microstructural evolution and its impact on battery performance is pivotal for optimizing porous Zn anodes. By using *in situ* atomic-scale characterization techniques, such as *in situ* electrochemical fluorescence microscopy, *in situ* electrochemical Raman spectroscopy, atomic force microscopy, and transmission electron microscopy, the electrochemical reaction process related to porous Zn anodes can be observed real time. In addition, the transport mechanism of Zn^{2+} ions between the electrodes and the electrolyte can be elucidated, providing key information for optimizing the material design and battery performance. Through surface and interface analysis (e.g., X-ray photoelectron spectroscopy, electrochemical impedance spectroscopy, and neutron diffraction), the surface composition, chemical state, and morphology of porous Zn anodes can be obtained, enabling a comprehensive understanding of the surface electrochemical properties and interfacial reaction characteristics of AZIBs. Moreover, differential scanning calorimetry and thermal gravimetric analysis can be used to study the thermal stability, phase behavior, and thermal decomposition characteristics of porous Zn anodes, which provides valuable insights into battery safety assessment and material design.

3. System integration and practical evaluation. The system integration design of AZIBs is an important direction for their future development, requiring the optimization of electrolyte formulation, battery components, and module design to achieve higher energy density, longer cycle life, and improved safety features. The majority of previous research work in the field of Zn anodes has emphasized cycling life as a key performance indicator. Although this indicator can be remarkably improved by incorporating excess Zn, standardized test parameters for battery cycling evaluation are lacking, such as current density, N/P ratio, and DOD. In particular, the areal capacity of cathodes is generally constrained to less than 0.5 mAh cm^{-2} to achieve high-multiplicity performance, resulting in low Zn utilization and a reduced mass energy density of the AZIBs.

Furthermore, the current production of porous Zn anodes typically involves complex manufacturing steps, thereby increasing production cost. Most of the meticulously considered designs, especially those involving gradient porous anodes, are not yet amenable to large-scale production. Consequently,

清華大學出版社 Tsinghua University Press | SciOpen

developing cost-effective and scalable methods for fabricating porous Zn anodes is crucial. In addition, assessing the battery performance under practical conditions is necessary to promote the practical applications of AZIBs.

Despite the need for further improvement with regard to battery cycle life, porous Zn anodes present distinct advantages, including the alleviation of local current density, uniformization of ion flux, and mitigation of volume expansion. The integration of advanced scientific investigations with engineering optimization strategies can facilitate the practical implementation of porous Zn anodes for high-performance AZIBs (Fig. 12).

Acknowledgements

Yao Wang would like to acknowledge the support from National Natural Science Foundation of China (Grant No. 22309102) and China Postdoctoral Science Foundation (Grant No. 2022M711788). Dong Zhou would like to acknowledge the support from National Key Research and Development Program of China (Grant No. 2022YFB2404500) and Fundamental Research Project of Shenzhen (Grant No. JCYJ20230807111702005). Guoxiu Wang would like to acknowledge the support from the Australian Research Council (ARC) through the ARC Discovery Project (Grant No. DP230101579) and ARC Linkage Project (Grant No. LP200200926).

Author contribution statement

Yichen Ding and Bingyue Ling are responsible for writing the original drafts. Xin Zhao, Xu Yang and Yao Wang contributed greatly to the review and revision of the article. Dong Zhou and Guoxiu Wang took the oversight and leadership responsibility for the whole process. All the authors have approved the final manuscript.

Data availability

Not applicable.

Declaration of competing interest

All the contributing authors report no conflict of interests in this work.

Funding

This work is granted by National Natural Science Foundation of China (Grant No. 22309102), China Postdoctoral Science Foundation (Grant No.

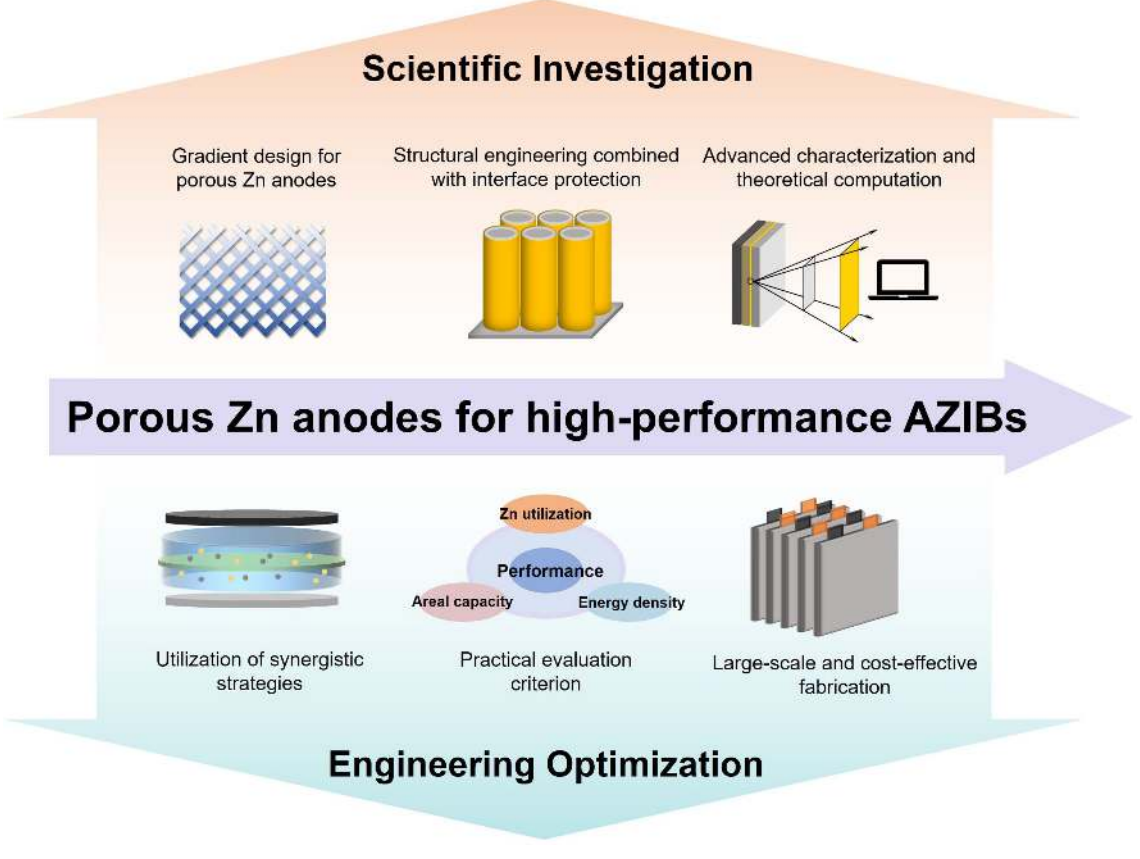

Figure 12 Future research directions associated with the development of advanced porous Zn metal anodes for high-performance AZIBs.

2022M711788), National Key Research and Development Program of China (Grant No. 2022YFB2404500), Fundamental Research Project of Shenzhen (Grant No. JCYJ20230807111702005), the Australian Research Council through the ARC Discovery Project (Grant No. DP230101579) and ACR Linkage Project (Grant No. LP200200926).

Use of AI statement

None.

References

[1] Yan, J. P., Ang, E. H., Yang, Y., Zhang, Y. F., Ye, M. H., Du, W. C., Li, C. C. (2021). High-voltage zinc-ion batteries: Design strategies and challenges. *Adv. Funct. Mater.* 31, 2010213.

[2] Dunn, B., Kamath, H., Tarascon, J. M. (2011). Electrical energy storage for the grid: a battery of choices. *Science* 334, 928–935.

[3] Zhu, Z. X., Jiang, T. L., Ali, M., Meng, Y. H., Jin, Y., Cui, Y., Chen, W. (2022). Rechargeable batteries for grid scale energy storage. *Chem. Rev.* 122, 16610–16751.

[4] Ni, Q., Kim, B., Wu, C., Kang, K. (2022). Non-electrode components for rechargeable aqueous zinc batteries: Electrolytes, solid-electrolyte-interphase, current collectors, binders, and separators. *Adv. Mater.* 34, 2108206.

[5] Li, Y., Wu, F., Li, Y., Liu, M. Q., Feng, X., Bai, Y., Wu, C. (2022). Ether-based electrolytes for sodium ion batteries. *Chem. Soc. Rev.* 51, 4484–4536.

[6] Li, H. F., Ma, L. T., Han, C. P., Wang, Z. F., Liu, Z. X., Tang, Z. J., Zhi, C. Y. (2019). Advanced rechargeable zinc-based batteries: Recent progress and future perspectives. *Nano Energy* 62, 550–587.

[7] Xu, C. J., Li, B. H., Du, H. D., Kang, F. Y. (2012). Energetic zinc ion chemistry: The rechargeable zinc ion battery. *Angew. Chem. Int. Ed.* 51, 933–935.

[8] Gourley, S. W. D., Brown, R., Adams, B. D., Higgins, D. (2023). Zinc-ion batteries for stationary energy storage. *Joule* 7, 1415–1436.

[9] Yu, X. H., Li, Z. G., Wu, X. H., Zhang, H. T., Zhao, Q. G., Liang, H. F., Wang, H., Chao, D. L., Wang, F., Qiao, Y., et al. (2023). Ten concerns of Zn metal anode for rechargeable aqueous zinc batteries. *Joule* 7, 1145–1175.

[10] Chen, J. Y., Wang, Y. Z., Tian, Z. N., Zhao, J., Ma, Y. W., Alshareef, H. N. (2024). Recent developments in three-dimensional Zn metal anodes for battery applications. *InfoMat* 6, e12485.

[11] Guo, N., Huo, W. J., Dong, X. Y., Sun, Z. F., Lu, Y. T., Wu, X. W., Dai, L., Wang, L., Lin, H. C., Liu, H. D., et al. (2022). A review on 3D zinc anodes for zinc ion batteries. *Small Methods* 6, 2200597.

[12] Tian, H., Yang, J. L., Deng, Y. R., Tang, W. H., Liu, R. P., Xu, C. Y., Han, P., Fan, H. J. (2023). Steel anti-corrosion strategy enables long-cycle Zn anode. *Adv. Energy Mater.* 13, 2202603.

[13] Wang, Y., Wang, T. R., Bu, S. Y., Zhu, J. X., Wang, Y. B., Zhang, R., Hong, H., Zhang, W. J., Fan, J., Zhi, C. Y. (2023). Sulfolane-containing aqueous electrolyte solutions for producing efficient ampere-hour-level zinc metal battery pouch cells. *Nat. Commun.* 14, 1828.

[14] Feng, D. D., Jiao, Y. C., Wu, P. Y. (2023). Guiding Zn uniform deposition with polymer additives for long-lasting and highly utilized Zn metal anodes. *Angew. Chem., Int. Ed.* 62, e202314456.

[15] Xie, X. S., Liang, S. Q., Gao, J. W., Guo, S., Guo, J. B., Wang, C., Xu, G. Y., Wu, X. W., Chen, G., Zhou, J. (2020). Manipulating the ion-transfer kinetics and interface stability for high-performance zinc metal anodes. *Energy Environ. Sci.* 13, 503–510.

[16] Sun, G. Q., Zhou, M. Q., Dong, X. Y., Zang, S. Q., Qu, L. T. (2022). An efficient and versatile biopolishing strategy to construct high performance zinc anode. *Nano Res.* 15, 5081–5088.

[17] Li, X. L., Li, Q., Hou, Y., Yang, Q., Chen, Z., Huang, Z. D., Liang, G. J., Zhao, Y. W., Ma, L. T., Li, M., et al. (2021). Toward a practical Zn powder anode: $Ti_3C_2T_x$ MXene as a lattice-match electrons/ions redistributor. *ACS Nano* 15, 14631–14642.

[18] Na, Z., Qi, H. K., Li, S. H., Wu, Y. B., Wang, Q. S., Huang, G. (2023). Stable zinc metal anode by nanosecond pulsed laser enabled gradient design. *ACS Energy Lett.* 8, 3297–3306.

[19] Wang, T. Q., Tang, Y., Yu, M. X., Lu, B. G., Zhang, X. T., Zhou, J. (2023). Spirally grown zinc-cobalt alloy layer enables highly reversible zinc metal anodes. *Adv. Funct. Mater.* 33, 2306101.

[20] Cao, Q. H., Gao, Y., Pu, J., Zhao, X., Wang, Y. X., Chen, J. P., Guan, C. (2023). Gradient design of imprinted anode for stable Zn-ion batteries. *Nat. Commun.* 14, 641.

[21] Xue, P., Guo, C., Li, L., Li, H. P., Luo, D., Tan, L. C., Chen, Z. W. (2022). A MOF-derivative decorated hierarchical porous host enabling ultrahigh rates and superior long-term cycling of dendrite-free Zn metal anodes. *Adv. Mater.* 34, 2110047.

[22] Zeng, L., He, J., Yang, C. Y., Luo, D., Yu, H. B., He, H. N., Zhang, C. H. (2023). Direct 3D printing of stress-released Zn powder anodes toward flexible dendrite-free Zn batteries. *Energy Storage Mater.* 54, 469–477.

[23] Parker, J. F., Chervin, C. N., Pala, I. R., Machler, M., Burz, M. F., Long, J. W., Rolison, D. R. (2017). Rechargeable nickel-3D zinc batteries: An energy-dense, safer alternative to lithium-ion. *Science* 356, 415–418.

[24] Li, P. P., Jin, Z. Y., Xiao, D. (2018). Three-dimensional nanotube-array anode enables a flexible Ni/Zn fibrous battery to ultrafast charge and discharge in seconds. *Energy Storage Mater.* 12, 232–240.

[25] Zeng, Y. X., Zhang, X. Y., Qin, R. F., Liu, X. Q., Fang, P. P., Zheng, D. Z., Tong, Y. X., Lu, X. H. (2019). Dendrite-free zinc deposition induced by multifunctional CNT frameworks for stable flexible Zn-ion batteries. *Adv. Mater.* 31, 1903675.

[26] Wang, S. B., Ran, Q., Yao, R. Q., Shi, H., Wen, Z., Zhao, M., Lang, X. Y., Jiang, Q. (2020). Lamella-nanostruc-

清華大學出版社 Tsinghua University Press | SciOpen

tured eutectic zinc–aluminum alloys as reversible and dendrite-free anodes for aqueous rechargeable batteries. *Nat. Commun.* 11, 1634.

[27] Kim, J. Y., Liu, G. C., Shim, G. Y., Kim, H., Lee, J. K. (2020). Functionalized Zn@ZnO hexagonal pyramid array for dendrite-free and ultrastable zinc metal anodes. *Adv. Funct. Mater.* 30, 2004210.

[28] Liu, H. Z., Li, J. H., Zhang, X. N., Liu, X. X., Yan, Y., Chen, F. J., Zhang, G. H., Duan, H. G. (2021). Ultrathin and ultralight Zn micromesh-induced spatial-selection deposition for flexible high-specific-energy Zn-ion batteries. *Adv. Funct. Mater.* 31, 2106550.

[29] Yang, Y., Liu, C. Y., Lv, Z. H., Yang, H., Zhang, Y. F., Ye, M. H., Chen, L. B., Zhao, J. B., Li, C. C. (2021). Synergistic manipulation of Zn^{2+} ion flux and desolvation effect enabled by anodic growth of a 3D ZnF_2 matrix for long-lifespan and dendrite-free Zn metal anodes. *Adv. Mater.* 33, 2007388.

[30] Zhang, M., Yu, P. F., Xiong, K. R., Wang, Y. Y., Liu, Y. L., Liang, Y. R. (2022). Construction of mixed ionic-electronic conducting scaffolds in Zn powder: A scalable route to dendrite-free and flexible Zn anodes. *Adv. Mater.* 34, 2200860.

[31] Gao, Y., Cao, Q. H., Pu, J., Zhao, X., Fu, G. W., Chen, J. P., Wang, Y. X., Guan, C. (2023). Stable Zn anodes with triple gradients. *Adv. Mater.* 35, 2207573.

[32] Mu, Y. B., Li, Z., Wu, B. K., Huang, H. D., Wu, F. H., Chu, Y. Q., Zou, L. F., Yang, M., He, J. F., Ye, L., et al. (2023). 3D hierarchical graphene matrices enable stable Zn anodes for aqueous Zn batteries. *Nat. Commun.* 14, 4205.

[33] Chazalviel, J. N. (1990). Electrochemical aspects of the generation of ramified metallic electrodeposits. *Phys. Rev. A* 42, 7355–7367.

[34] Hou, Z., Gao, Y., Zhou, R., Zhang, B. (2022). Unraveling the rate-dependent stability of metal anodes and its implication in designing cycling protocol. *Adv. Funct. Mater.* 32, 2107584.

[35] Zheng, X. Y., Huang, L. Q., Ye, X. L., Zhang, J. X., Min, F. Y., Luo, W., Huang, Y. H. (2021). Critical effects of electrolyte recipes for Li and Na metal batteries. *Chem* 7, 2312–2346.

[36] Li, B., Liu, S. D., Geng, Y. F., Mao, C. W., Dai, L., Wang, L., Jun, S. C., Lu, B. G., He, Z. X., Zhou, J. (2024). Achieving stable zinc metal anode via polyaniline interface regulation of Zn ion flux and desolvation. *Adv. Funct. Mater.* 34, 2214033.

[37] Du, Z. J., Wood, D. L., Daniel, C., Kalnaus, S., Li, J. L. (2017). Understanding limiting factors in thick electrode performance as applied to high energy density Li-ion batteries. *J. Appl. Electrochem.* 47, 405–415.

[38] Wu, J. Y., Ju, Z. Y., Zhang, X., Marschilok, A. C., Takeuchi, K. J., Wang, H. L., Takeuchi, E. S., Yu, G. H. (2022). Gradient design for high-energy and high-power batteries. *Adv. Mater.* 34, 2202780.

[39] Cao, R., Zhu, L. Q., Liu, H. C., Yang, W., Li, W. P. (2015). The effect of silica sols on electrodeposited zinc coatings for sintered ndfeb. *RSC Adv.* 5, 104375–104385.

[40] Wang, X., Meng, J. P., Lin, X. G., Yang, Y. D., Zhou, S., Wang, Y. P., Pan, A. Q. (2021). Stable zinc metal anodes with textured crystal faces and functional zinc compound coatings. *Adv. Funct. Mater.* 31, 2106114.

[41] He, H. N., Zeng, L., Luo, D., He, J., Li, X. L., Guo, Z. P., Zhang, C. H. (2023). 3D printing of electron/ion-flux dual-gradient anodes for dendrite-free zinc batteries. *Adv. Mater.* 35, 2211498.

[42] Wang, X., Zeng, W., Hong, L., Xu, W. W., Yang, H. K., Wang, F., Duan, H. G., Tang, M., Jiang, H. Q. (2018). Stress-driven lithium dendrite growth mechanism and dendrite mitigation by electroplating on soft substrates. *Nat. Energy* 3, 227–235.

[43] Wang, C. C., Zhu, G. Y., Liu, P., Chen, Q. (2020). Monolithic nanoporous Zn anode for rechargeable alkaline batteries. *ACS Nano* 14, 2404–2411.

[44] Chamoun, M., Hertzberg, B. J., Gupta, T., Davies, D., Bhadra, S., Van Tassell, B., Erdonmez, C., Steingart, D. A. (2015). Hyper-dendritic nanoporous zinc foam anodes. *NPG Asia Mater.* 7, e178.

[45] Zhang, Y. R., Han, X. P., Liu, R. Z., Yang, Z. X., Zhang, S. J., Zhang, Y. M., Wang, H. L., Cao, Y., Chen, A., Sun, J. (2022). Manipulating the zinc deposition behavior in hexagonal patterns at the preferential Zn(100) crystal plane to construct surficial dendrite-free zinc metal anode. *Small* 18, 2105978.

[46] Li, F., Ma, D. T., Ouyang, K. F., Yang, M., Qiu, J. M., Feng, J., Wang, Y. Y., Mi, H. W., Sun, S. C., Sun, L. N., et al. (2023). A theory-driven complementary interface effect for fast-kinetics and ultrastable Zn metal anodes in aqueous/solid electrolytes. *Adv. Energy Mater.* 13, 2204365.

[47] Xu, D. M., Chen, B. Q., Ren, X. T., Han, C., Chang, Z., Pan, A. Q., Zhou, H. S. (2024). Selectively etching-off the highly reactive (002) Zn facet enables highly efficient aqueous zinc-metal batteries. *Energy Environ. Sci.* 2, 642–654.

[48] Wang, J. D., Cai, Z., Xiao, R., Ou, Y. T., Zhan, R. M., Yuan, Z., Sun, Y. M. (2020). A chemically polished zinc metal electrode with a ridge-like structure for cycle-stable aqueous batteries. *ACS Appl. Mater. Interfaces* 12, 23028–23034.

[49] Fu, H., Wen, Q., Li, P. Y., Wang, Z. Y., He, Z. J., Yan, C., Mao, J., Dai, K. H., Zhang, X. H., Zheng, J. C. (2022). In-situ chemical conversion film for stabilizing zinc metal anodes. *J. Energy Chem.* 73, 387–393.

[50] Deng, C. B., Li, Y., Liu, S. J., Yang, J. L., Huang, B. L., Liu, J. P., Huang, J. Q. (2023). Nature-inspired interfacial engineering for highly stable Zn metal anodes. *Energy Storage Mater.* 58, 279–286.

[51] Lv, L. L., Wu, X. C., Han, X. S., Li, C. X. (2020). Amino acid modified graphene oxide for assembly of nanoparticles for wastewater treatment. *Appl. Surf. Sci.* 534, 147620.

[52] Wen, Q., Fu, H., Wang, Z. Y., Huang, Y. D., He, Z. J., Yan, C., Mao, J., Dai, K. H., Zhang, X. H., Zheng, J. C.

(2022). A hydrophobic layer of amino acid enabling dendrite-free Zn anodes for aqueous zinc-ion batteries. *J. Mater. Chem. A* 10, 17501–17510.

[53] Wang, W. X., Huang, G., Wang, Y. Z., Cao, Z., Cavallo, L., Hedhili, M. N., Alshareef, H. N. (2022). Organic acid etching strategy for dendrite suppression in aqueous zinc-ion batteries. *Adv. Energy Mater.* 12, 2102797.

[54] Zhao, R. Z., Dong, X. S., Liang, P., Li, H. P., Zhang, T. S., Zhou, W. H., Wang, B. Y., Yang, Z. D., Wang, X., Wang, L. P., et al. (2023). Prioritizing hetero-metallic interfaces via thermodynamics inertia and kinetics zincophilia metrics for tough Zn-based aqueous batteries. *Adv. Mater.* 35, 2209288.

[55] Jiao, Q. Y., Zhai, X. W., Sun, Z. X., Wang, W. J., Liu, S. H., Ding, H., Chu, W. S., Zhou, M., Wu, C. Z. (2023). Ultrafast superfilling construction of a metal artificial interface for long-term stable zinc anodes. *Adv. Mater.* 35, 2300850.

[56] Chen, J. Y., Qiao, X., Han, X. R., Zhang, J. H., Wu, H. B., He, Q., Chen, Z. B., Shi, L., Wang, Y. Z., Xie, Y. N., et al. (2022). Releasing plating-induced stress for highly reversible aqueous Zn metal anodes. *Nano Energy* 103, 107814.

[57] Bie, Z., Yang, Q., Cai, X. X., Chen, Z., Jiao, Z. Y., Zhu, J. B., Li, Z. F., Liu, J. Z., Song, W. X., Zhi, C. Y. (2022). One-step construction of a polyporous and zincophilic interface for stable zinc metal anodes. *Adv. Energy Mater.* 12, 2202683.

[58] Nayaka, G. P., Zhang, Y. J., Dong, P., Wang, D., Zhou, Z. R., Duan, J. G., Li, X., Lin, Y., Meng, Q., Pai, K. V., et al. (2019). An environmental friendly attempt to recycle the spent Li-ion battery cathode through organic acid leaching. *J. Environ. Chem. Eng.* 7, 102854.

[59] Li, J. J., Liu, Z. X., Han, S. H., Zhou, P., Lu, B. G., Zhou, J. D., Zeng, Z. Y., Chen, Z. Z., Zhou, J. (2023). Hetero nucleus growth stabilizing zinc anode for high-biosecurity zinc-ion batteries. *Nano-Micro Lett.* 15, 237.

[60] Zou, Y. H., Su, Y. W., Qiao, C. P., Li, W. P., Xue, Z. K., Yang, X. Z., Lu, M. Y., Guo, W. Y., Sun, J. Y. (2023). A generic "engraving in aprotic medium" strategy toward stabilized Zn anodes. *Adv. Energy Mater.* 13, 2300932.

[61] Zhang, X. T., Li, J. X., Liu, Y. F., Lu, B. G., Liang, S. Q., Zhou, J. (2024). Single [0001]-oriented zinc metal anode enables sustainable zinc batteries. *Nat. Commun.* 15, 2735.

[62] Hong, L., Wang, L. Y., Wang, Y. L., Wu, X. M., Huang, W., Zhou, Y. F., Wang, K. X., Chen, J. S. (2022). Toward hydrogen-free and dendrite-free aqueous zinc batteries: Formation of zincophilic protective layer on Zn anodes. *Adv. Sci*. (*Weinh*.) 9, 2104866.

[63] Ouyang, K. F., Ma, D. T., Zhao, N., Wang, Y. Y., Yang, M., Mi, H. W., Sun, L. N., He, C. X., Zhang, P. X. (2022). A new insight into ultrastable Zn metal batteries enabled by in situ built multifunctional metallic interphase. *Adv. Funct. Mater.* 32, 2109749.

[64] He, P., Huang, J. X. (2022). Chemical passivation stabilizes Zn anode. *Adv. Mater.* 34, 2109872.

[65] Zhang, L., Zhang, B., Zhang, T., Li, T., Shi, T. F., Li, W., Shen, T., Huang, X. X., Xu, J. J., Zhang, X. G., et al. (2021). Eliminating dendrites and side reactions via a multifunctional ZnSe protective layer toward advanced aqueous Zn metal batteries. *Adv. Funct. Mater.* 31, 2100186.

[66] Huang, Y. F., Chang, Z. W., Liu, W. B., Huang, W. T., Dong, L. B., Kang, F. Y., Xu, C. J. (2022). Layer-by-layer zinc metal anodes to achieve long-life zinc-ion batteries. *Chem. Eng. J.* 431, 133902.

[67] Zhang, Q., Luan, J. Y., Fu, L., Wu, S. G., Tang, Y. B., Ji, X., Wang, H. Y. (2019). The three-dimensional dendrite-free zinc anode on a copper mesh with a zinc-oriented polyacrylamide electrolyte additive. *Angew. Chem. Int. Ed.* 58, 15841–15847.

[68] Shi, X. D., Xu, G. F., Liang, S. Q., Li, C. P., Guo, S., Xie, X. S., Ma, X. M., Zhou, J. (2019). Homogeneous deposition of zinc on three-dimensional porous copper foam as a superior zinc metal anode. *ACS Sustainable Chem. Eng.* 7, 17737–17746.

[69] Kang, Z., Wu, C. L., Dong, L. B., Liu, W. B., Mou, J., Zhang, J. W., Chang, Z. W., Jiang, B. Z., Wang, G. X., Kang, F. Y., et al. (2019). 3D porous copper skeleton supported zinc anode toward high capacity and long cycle life zinc ion batteries. *ACS Sustainable Chem. Eng.* 7, 3364–3371.

[70] An, Y. L., Tian, Y., Xiong, S. L., Feng, J. K., Qian, Y. T. (2021). Scalable and controllable synthesis of interface-engineered nanoporous host for dendrite-free and high rate zinc metal batteries. *ACS Nano* 15, 11828–11842.

[71] Yi, Z. H., Liu, J. X., Tan, S. D., Sang, Z. Y., Mao, J., Yin, L. C., Liu, X. G., Wang, L. Q., Hou, F., Dou, S. X., et al. (2022). An ultrahigh rate and stable zinc anode by facet-matching-induced dendrite regulation. *Adv. Mater.* 34, 2203835.

[72] Fan, X. Y., Yang, H., Feng, B., Zhu, Y. Q., Wu, Y., Sun, R. B., Gou, L., Xie, J., Li, D. L., Ding, Y. L. (2022). Rationally designed In@Zn@In trilayer structure on 3D porous Cu towards high-performance Zn-ion batteries. *Chem. Eng. J.* 445, 136799.

[73] Yu, H. M., Li, Q. Y., Liu, W., Wang, H., Ni, X. Y., Zhao, Q. W., Wei, W. F., Ji, X. B., Chen, Y. J., Chen, L. B. (2022). Fast ion diffusion alloy layer facilitating 3D mesh substrate for dendrite-free zinc-ion hybrid capacitors. *J. Energy Chem.* 73, 565–574.

[74] Douka, A. I., Xu, Y. Y., Yang, H., Zaman, S., Yan, Y., Liu, H. F., Salam, M. A., Xia, B. Y. (2020). A zeolitic-imidazole frameworks-derived interconnected macroporous carbon matrix for efficient oxygen electrocatalysis in rechargeable zinc–air batteries. *Adv. Mater.* 32, 2002170.

[75] Pan, Y. L., Hu, M., Ma, M. D., Li, Z. H., Gao, Y. F., Xiong, M., Gao, G. Y., Zhao, Z. S., Tian, Y. J., Xu, B., et al. (2017). Multithreaded conductive carbon: 1d conduction in 3D carbon. *Carbon* 115, 584–588.

[76] Borchardt, L., Zhu, Q. L., Casco, M. E., Berger, R., Zhuang, X. D., Kaskel, S., Feng, X. L., Xu, Q. (2017). Toward a molecular design of porous carbon materials.

Mater. Today 20, 592–610.

[77] Zheng, J. X., Zhao, Q., Tang, T., Yin, J. F., Quilty, C. D., Renderos, G. D., Liu, X. T., Deng, Y., Wang, L., Bock, D. C., et al. (2019). Reversible epitaxial electrodeposition of metals in battery anodes. *Science* 366, 645–648.

[78] Xie, F. X., Li, H., Wang, X. S., Zhi, X., Chao, D. L., Davey, K., Qiao, S. Z. (2021). Mechanism for zincophilic sites on zinc-metal anode hosts in aqueous batteries. *Adv. Energy Mater.* 11, 2003419.

[79] Wang, J. H., Chen, L. F., Dong, W. X., Zhang, K. L., Qu, Y. F., Qian, J. W., Yu, S. H. (2023). Three-dimensional zinc-seeded carbon nanofiber architectures as lightweight and flexible hosts for a highly reversible zinc metal anode. *ACS Nano* 17, 19087–19097.

[80] Zhou, J. H., Xie, M., Wu, F., Mei, Y., Hao, Y. T., Li, L., Chen, R. J. (2022). Encapsulation of metallic Zn in a hybrid MXene/graphene aerogel as a stable Zn anode for foldable Zn-ion batteries. *Adv. Mater.* 34, 2106897.

[81] Cao, Q. H., Gao, H., Gao, Y., Yang, J., Li, C., Pu, J., Du, J. J., Yang, J. J., Cai, D. M., Pan, Z. H., et al. (2021). Regulating dendrite-free zinc deposition by 3D zincopilic nitrogen-doped vertical graphene for high-performance flexible Zn-ion batteries. *Adv. Funct. Mater.* 31, 2103922.

[82] Wang, Q., Astruc, D. (2020). State of the art and prospects in metal–organic framework (MOF)-based and MOF-derived nanocatalysis. *Chem. Rev.* 120, 1438–1511.

[83] Wang, Z., Xu, J., Yang, J. H., Xue, Y. H., Dai, L. M. (2022). Ultraviolet/ozone treatment for boosting oer activity of MOF nanoneedle arrays. *Chem. Eng. J.* 427, 131498.

[84] Yuksel, R., Buyukcakir, O., Seong, W. K., Ruoff, R. S. (2020). Metal-organic framework integrated anodes for aqueous zinc-ion batteries. *Adv. Energy Mater.* 10, 1904215.

[85] Yu, H., Yao, H. X., Zheng, Y. Q., Liu, D., Chen, J. S., Guo, Y., Li, N. W., Yu, L. (2024). Formation of hierarchical Zn/N-doped carbon hollow nanofibers towards dendrite-free Zn metal anodes. *Adv. Funct. Mater.* 34, 2311038.

[86] Gong, Y., Xue, Y. H. (2023). Carbon nanomaterials for stabilizing zinc anodes in zinc-ion batteries. *New Carbon Mater.* 38, 438–454.

[87] Tao, Y., Zuo, S. W., Xiao, S. H., Sun, P. X., Li, N. W., Chen, J. S., Zhang, H. B., Yu, L. (2022). Atomically dispersed Cu in zeolitic imidazolate framework nanoflake array for dendrite-free Zn metal anode. *Small* 18, 2203231.

[88] Li, H. P., Guo, C., Zhang, T. S., Xue, P., Zhao, R. Z., Zhou, W. H., Li, W., Elzatahry, A., Zhao, D. Y., Chao, D. L. (2022). Hierarchical confinement effect with zincophilic and spatial traps stabilized Zn-based aqueous battery. *Nano Lett.* 22, 4223–4231.

[89] Zeng, Y. H., Sun, P. X., Pei, Z. H., Jin, Q., Zhang, X. T., Yu, L., Lou, X. W. D. (2022). Nitrogen-doped carbon fibers embedded with zincophilic Cu nanoboxes for stable Zn-metal anodes. *Adv. Mater.* 34, 2200342.

[90] Yu, H., Zeng, Y. X., Li, N. W., Luan, D. Y., Yu, L., Lou, X. W. D. (2022). Confining Sn nanoparticles in interconnected N-doped hollow carbon spheres as hierarchical zincophilic fibers for dendrite-free Zn metal anodes. *Sci. Adv.* 8, eabm5766.

[91] Zhou, W. J., Wu, T., Chen, M. F., Tian, Q. H., Han, X., Xu, X. W., Chen, J. Z. (2022). Wood-based electrodes enabling stable, anti-freezing, and flexible aqueous zinc-ion batteries. *Energy Storage Mater.* 51, 286–293.

[92] Wang, R., Xin, S., Chao, D. L., Liu, Z. X., Wan, J. D., Xiong, P., Luo, Q. Q., Hua, K., Hao, J. N., Zhang, C. F. (2022). Fast and regulated zinc deposition in a semiconductor substrate toward high-performance aqueous rechargeable batteries. *Adv. Funct. Mater.* 32, 2207751.

[93] Li, Q., Wang, Y. B., Mo, F. N., Wang, D. H., Liang, G. J., Zhao, Y. W., Yang, Q., Huang, Z. D., Zhi, C. Y. (2021). Calendar life of Zn batteries based on Zn anode with Zn powder/current collector structure. *Adv. Energy Mater.* 11, 2003931.

[94] Li, S. P., Wang, H., Cuthbert, J., Liu, T., Whitacre, J. F., Matyjaszewski, K. (2019). A semiliquid lithium metal anode. *Joule* 3, 1637–1646.

[95] Liu, Q., Yu, Z. L., Zhou, R., Zhang, B. (2023). A semi-liquid electrode toward stable Zn powder anode. *Adv. Funct. Mater.* 33, 2210290.

[96] Hu, Q., Hou, J. M., Liu, Y. B., Li, L., Ran, Q. W., Mao, J. Q., Liu, X. Q., Zhao, J. X., Pang, H. (2023). Modulating zinc metal reversibility by confined antifluctuator film for durable and dendrite-free zinc ion batteries. *Adv. Mater.* 2303336.

[97] Wang, J. X., Zhang, H., Yang, L. Z., Zhang, S. Y., Han, X. P., Hu, W. B. (2024). *In situ* implanting 3D carbon network reinforced zinc composite by powder metallurgy for highly reversible Zn-based battery anodes. *Angew. Chem. Int. Ed.* 63, e202318149.

[98] Yang, Z. F., Zhang, Q., Li, W. B., Xie, C. L., Wu, T. Q., Hu, C., Tang, Y. G., Wang, H. Y. (2023). A semi-solid zinc powder-based slurry anode for advanced aqueous zinc-ion batteries. *Angew. Chem. Int. Ed.* 62, e202215306.

[99] Cao, C. H., Zhou, K. Q., Du, W. C., Li, C. C., Ye, M. H., Zhang, Y. F., Tang, Y. C., Liu, X. Q. (2023). Designing soft solid-like viscoelastic zinc powder anode toward high-performance aqueous zinc-ion batteries. *Adv. Energy Mater.* 13, 2301835.

[100] Du, Y. X., Chi, X. W., Huang, J. Q., Qiu, Q. L., Liu, Y. (2020). Long lifespan and high-rate Zn anode boosted by 3D porous structure and conducting network. *J. Power Sources* 479, 228808.

[101] Du, W. C., Huang, S., Zhang, Y. F., Ye, M. H., Li, C. C. (2022). Enable commercial zinc powders for dendrite-free zinc anode with improved utilization rate by pristine graphene hybridization. *Energy Storage Mater.* 45, 465–473.

[102] Huyan, X. D., Yi, Z. H., Sang, Z. Y., Tan, S. D., Liu, J. X., Chen, R., Si, W. P., Liang, J., Hou, F. (2023). Polyethylene glycol coating on zinc powder surface: Applications in dendrite-free zinc anodes with enhanced utilization rate. *Appl. Surf. Sci.* 614, 156209.

[103] Chen, H. L., Zhang, W. Y., Yi, S., Su, Z., Zhao, Z. Q., Zhang, Y. Y., Niu, B., Long, D. H. (2024). Zinc iso-plating/stripping: Toward a practical Zn powder anode with ultra-long life over 5600 h. *Energy Environ. Sci.* 17, 3146–3156.

[104] Lin, Y. H., Hu, Y. Z., Zhang, S., Xu, Z. Q., Feng, T. T., Zhou, H. P., Wu, M. Q. (2022). Binder-free freestanding 3D Zn-graphene anode induced from commercial zinc powders and graphene oxide for zinc ion battery with high utilization rate. *ACS Appl. Energy Mater.* 5, 15222–15232.

[105] Xu, X. Y., Li, S. M., Cao, Z. J., Yang, S. B., Li, B. (2024). Boosting ion diffusion and charge transfer by zincophilic accordion arrays to achieve ultrafast aqueous zinc metal batteries. *Adv. Energy Mater.* 14, 2303971.

[106] Rehnlund, D., Wang, Z. H., Nyholm, L. (2022). Lithium-diffusion induced capacity losses in lithium-based batteries. *Adv. Mater.* 34, 2108827.

[107] Zhang, Y. Y., Malyi, O. I., Tang, Y. X., Wei, J. Q., Zhu, Z. Q., Xia, H. R., Li, W. L., Guo, J., Zhou, X. R., Chen, Z., et al. (2017). Reducing the charge carrier transport barrier in functionally layer-graded electrodes. *Angew. Chem. Int. Ed.* 56, 14847–14852.

[108] Ju, Z. Y., Zhang, X., Wu, J. Y., Yu, G. H. (2021). Vertically aligned two-dimensional materials-based thick electrodes for scalable energy storage systems. *Nano Res.* 14, 3562–3575.

[109] Ju, Z. Y., Zhu, Y., Zhang, X., Lutz, D. M., Fang, Z. W., Takeuchi, K. J., Takeuchi, E. S., Marschilok, A. C., Yu, G. H. (2020). Understanding thickness-dependent transport kinetics in nanosheet-based battery electrodes. *Chem. Mater.* 32, 1684–1692.

[110] Cao, Q. H., Pan, Z. H., Gao, Y., Pu, J., Fu, G. W., Cheng, G. H., Guan, C. (2022). Stable imprinted zincophilic Zn anodes with high capacity. *Adv. Funct. Mater.* 32, 2205771.

[111] Huang, Z. C., Li, H. Y., Yang, Z., Wang, H. Z., Ding, J. N., Xu, L. Y., Tian, Y. L., Mitlin, D., Ding, J., Hu, W. B. (2022). Nanosecond laser lithography enables concave-convex zinc metal battery anodes with ultrahigh areal capacity. *Energy Storage Mater.* 51, 273–285.

[112] Liang, G. J., Zhu, J. X., Yan, B. X., Li, Q., Chen, A., Chen, Z., Wang, X. Q., Xiong, B., Fan, J., Xu, J., et al. (2022). Gradient fluorinated alloy to enable highly reversible Zn-metal anode chemistry. *Energy Environ. Sci.* 15, 1086–1096.

[113] Gao, X. J., Yang, X. F., Adair, K., Li, X. N., Liang, J. W., Sun, Q., Zhao, Y., Li, R. N., Sham, T. K., Sun, X. L. (2020). 3D vertically aligned li metal anodes with ultrahigh cycling currents and capacities of 10 mA cm^{-2} 20 mAh cm^{-2} realized by selective nucleation within microchannel walls. *Adv. Energy Mater.* 10, 1903753.

[114] Li, S. Y., Fu, J., Miao, G. X., Wang, S. P., Zhao, W. Y., Wu, Z. C., Zhang, Y. J., Yang, X. W. (2021). Toward planar and dendrite-free Zn electrodepositions by regulating Sn-crystal textured surface. *Adv. Mater.* 33, 2008424.

[115] Zhang, G. H., Zhang, X. N., Liu, H. Z., Li, J. H., Chen, Y. Q., Duan, H. (2021). 3D-printed multi-channel metal lattices enabling localized electric-field redistribution for dendrite-free aqueous Zn ion batteries. *Adv. Energy Mater.* 11, 2003927.

[116] Sun, P. X., Cao, Z. J., Zeng, Y. X., Xie, W. W., Li, N. W., Luan, D. Y., Yang, S. B., Yu, L., Lou, X. W. D. (2022). Formation of super-assembled TiO_x/Zn/N-doped carbon inverse opal towards dendrite-free Zn anodes. *Angew. Chem. Int. Ed.* 61, e202115649.

[117] Zeng, W., Wei, P. D., Chen, J. E., Wang, G. Z., Yan, Y., Yu, H. H., Yang, C. Y., Zhang, G. H., Jiang, H. Q. (2023). Ultra-stable zinc metal anodes enabled by uniform Zn deposition on a preferential crystal plane. *Adv. Energy Mater.* 13, 2302205.

[118] Idrees, M., Batool, S., Din, M. A. U., Javed, M. S., Ahmed, S., Chen, Z. W. (2023). Material-structure-property integrated additive manufacturing of batteries. *Nano Energy* 109, 108247.

[119] Chang, P., Mei, H., Zhou, S. X., Dassios, K. G., Cheng, L. F. (2019). 3D printed electrochemical energy storage devices. *J. Mater. Chem. A* 7, 4230–4258.

[120] Wu, B. K., Guo, B. B., Chen, Y. Z., Mu, Y. B., Qu, H. Q., Lin, M., Bai, J. M., Zhao, T. S., Zeng, L. (2023). High zinc utilization aqueous zinc ion batteries enabled by 3D printed graphene arrays. *Energy Storage Mater.* 54, 75–84.

[121] Zeng, L., He, H. N., Chen, H. Y., Luo, D., He, J., Zhang, C. H. (2022). 3D printing architecting reservoir-integrated anode for dendrite-free, safe, and durable Zn batteries. *Adv. Energy Mater.* 12, 2103708.

[122] Zhai, P. B., Wang, T. S., Jiang, H. N., Wan, J. Y., Wei, Y., Wang, L., Liu, W., Chen, Q., Yang, W. W., Cui, Y., et al. (2021). 3D artificial solid-electrolyte interphase for lithium metal anodes enabled by insulator-metal-insulator layered heterostructures. *Adv. Mater.* 33, 2006247.

[123] Cao, Z. J., Li, B., Yang, S. B. (2019). Dendrite-free lithium anodes with ultra-deep stripping and plating properties based on vertically oriented lithium-copper-lithium arrays. *Adv. Mater.* 31, 1901310.

[124] Qi, Y. B., Jang, T. J., Ramadesigan, V., Schwartz, D. T., Subramanian, V. R. (2017). Is there a benefit in employing graded electrodes for lithium-ion batteries. *J. Electrochem. Soc.* 164, A3196–A3207.

[125] Ramadesigan, V., Methekar, R. N., Latinwo, F., Braatz, R. D., Subramanian, V. R. (2010). Optimal porosity distribution for minimized ohmic drop across a porous electrode. *J. Electrochem. Soc.* 157, A1328–A1334.

[126] Zhao, X., Gao, Y., Cao, Q. H., Bu, F., Pu, J., Wang, Y. X., Guan, C. (2023). A high-capacity gradient Zn powder anode for flexible Zn-ion batteries. *Adv. Energy Mater.* 13, 2301741.

[127] Shen, Z. X., Luo, L., Li, C. W., Pu, J., Xie, J. P., Wang, L. T., Huai, Z., Dai, Z. Y., Yao, Y. G., Hong, G. (2021). Stratified zinc-binding strategy toward prolonged cycling and flexibility of aqueous fibrous zinc metal batteries. *Adv. Energy Mater.* 11, 2100214.

[128] Li, Y. M., Wang, Z. W., Li, W. H., Zhang, X. Y., Yin, C., Li, K., Guo, W., Zhang, J. P., Wu, X. L. (2023). Trinary

nanogradients at electrode/electrolyte interface for lean zinc metal batteries. *Energy Storage Mater.* 61, 102873.

[129] Lu, H. Y., Hu, J. S., Zhang, Y., Zhang, K. Q., Yan, X. Y., Li, H. Q., Li, J. Z., Li, Y. J., Zhao, J. X., Xu, B. G. (2023). 3D cold-trap environment printing for long-cycle aqueous Zn-ion batteries. *Adv. Mater.* 35, 2209886.

[130] Lu, H. Y., Hu, J. S., Zhang, K. Q., Zhao, J. X., Deng, S. Z., Li, Y. J., Xu, B. G., Pang, H. (2024). Microfluidic-assisted 3D printing zinc powder anode with 2D conductive mof/MXene heterostructures for high-stable zinc-organic battery. *Adv. Mater.* 36, 2309753.

[131] Yang, J. Y., Xu, X., Gao, Y., Wang, Y. X., Cao, Q. H., Pu, J., Bu, F., Meng, T., Guan, C. (2023). Ultra-stable 3D-printed Zn powder-based anode coated with a conformal ion-conductive layer. *Adv. Energy Mater.* 13, 2301997.

[132] Tian, H. J., Feng, G. X., Wang, Q., Li, Z., Zhang, W., Lucero, M., Feng, Z. X., Wang, Z. L., Zhang, Y. N., Zhen, C., et al. (2022). Three-dimensional Zn-based alloys for dendrite-free aqueous Zn battery in dual-cation electrolytes. *Nat. Commun.* 13, 7922.

[133] Li, G. P., Wang, X. L., Lv, S. H., Wang, J. X., Yu, W. S., Dong, X. T., Liu, D. T. (2023). In situ constructing a film-coated 3D porous Zn anode by iodine etching strategy toward horizontally arranged dendrite-free Zn deposition. *Adv. Funct. Mater.* 33, 2208288.

[134] Zhang, W. Y., Dong, M. Y., Jiang, K. R., Yang, D. L., Tan, X. H., Zhai, S. L., Feng, R. F., Chen, N., King, G., Zhang, H., et al. (2022). Self-repairing interphase reconstructed in each cycle for highly reversible aqueous zinc batteries. *Nat. Commun.* 13, 5348.

[135] Wang, D. D., Liu, H. X., Lv, D., Wang, C., Yang, J., Qian, Y. T. (2023). Rational screening of artificial solid electrolyte interphases on Zn for ultrahigh-rate and long-life aqueous batteries. *Adv. Mater.* 35, 2207908.